

Shared Community Energy Storage Allocation and Optimization

by

Hsiu-Chuan Chang

A thesis
presented to the University of Waterloo
in fulfillment of the
thesis requirement for the degree of
Master of Applied Science
in
Management Sciences

Waterloo, Ontario, Canada, 2019

© Hsiu-Chuan Chang 2019

Author's Declaration

I hereby declare that I am the sole author of this thesis. This is a true copy of the thesis, including any required final revisions, as accepted by my examiners.

I understand that my thesis may be made electronically available to the public.

Abstract

Distributed Energy Resources (DERs) have been playing an increasingly important role for managing households energy costs. DERs consist primarily of energy generation and storage systems utilized by individual households or shared among them as a community. This research proposes a framework to allocate shared energy storage within a community and to then optimize the operational cost of electricity using a mixed integer linear programming (MILP). The allocation options of energy storage include the option of private energy storage (PES) and three options of community energy storage (CES): random, diverse, and homogeneous allocation. With various load options of appliances, photovoltaic (PV) generation and energy storage set-ups, the operational cost of electricity for each household is minimized to provide the optimal operation scheduling.

In addition to the electricity operational cost, energy storage utilization, and operation fairness are used to compare different allocation options of storage systems. Computational results are presented on two real use cases: Waterloo, Canada and Ennis, Ireland. For each case, one typical summer day and one common winter day are selected to simulate different scenarios of the two seasons. Given the allocation options and ownership rates of residential energy storage deployment, this research shows the advantage of using CES as opposed to PES and evaluates the cost savings which can facilitate future deployment of CES.

Keywords: Community energy storage, distributed energy resources, smart energy community, optimization, allocation

Acknowledgements

I wish to express my sincere gratitude and appreciation to my supervisors Dr. Jatin Nathwani and Dr. Bissan Ghaddar, for their support during the course of my study. I would like to express my sincere gratefulness to my supervisor Dr. Bissan Ghaddar, for providing me this opportunity to work on this interesting research project, and also for her support and advice during my research and the writing of this thesis. Moreover, I would like to express my sincere thankfulness to my supervisor Dr. Jatin Nathwani, for his research guidance and support, and for his recommendation regarding my research funding and my future career direction. Furthermore, I sincerely thank Dr. Tristan de Wildt, for his extensive knowledge that he provided me and his valuable advice and comments during the course of my research. Also, I would like to thank the laboratory member Mr. Bo Lin, for helping me inspect and debug the code of this research.

I also would like to express my sincere thanks to Waterloo Institute for Sustainable Energy, for the fellowship which helped me continue my research. I also want to thank Dr. Frank Safayeni and Dr. Fatih Safa Erenay, for the support and advice of my teaching assistant job. In addition, I am thankful to Ms. Wendy Fleming, Ms. Lisa Hendel, and Ms. Kathy Tytko, for their administrative support in my studies.

Finally, I want to express my thanks to my friends in the Department of Management Sciences, Computer Science, and System Design Engineering, who always provided me with motivation, moral support, and academic advice throughout my study at the University of Waterloo.

Dedication

To my true love, Abby, and my cats, NaNa and NiNi

To my parents and my sister

Without you, I am nothing

Table of Contents

List of Figures	viii
List of Tables	xi
List of Symbols	xii
1 Introduction	1
1.1 Motivation	2
1.2 HEMS and DERs for a Single Household	4
1.3 Community in Smart Grid	7
1.3.1 The Concept of a Community	7
1.3.2 Sharing in a Community: Community Energy Storage	7
1.4 Thesis Objective	10
2 Solution Methodology	11
2.1 Community Setting	13
2.2 Allocating Energy Storage Systems	14
2.3 Operational Cost Optimization	16
2.4 Software and User Interface	22

3	Case Study	29
3.1	Case 1: Ennis, Ireland	30
3.1.1	Parameter Setting	30
3.1.2	Community Setting	34
3.1.3	Computational Results	35
3.1.3.1	Features for PES	35
3.1.3.2	Determining Battery Capacity of CES	38
3.1.3.3	Allocation Options for CES	42
3.2	Case 2: Waterloo, Canada	50
3.2.1	Parameter Setting	50
3.2.2	Community Setting	53
3.2.3	Computational Results	54
3.2.3.1	Features for PES	54
3.2.3.2	Determining Battery Capacity of CES	57
3.2.3.3	Allocation Options for CES	58
4	Conclusion	65
4.1	Summary and Conclusion	65
4.2	Future Work	67
	References	68

List of Figures

1.1	Electricity consumption in Ontario, Canada between 1962 and 2018.	2
1.2	HEMS and DERs in a single household.	4
1.3	Schematic diagram of CES in a community.	8
2.1	Flow chart of the solution approach.	12
2.2	Different allocation options of the CES.	15
2.3	An example for forming communities and allocations for CESs.	15
2.4	User interface.	22
2.5	User interface: initial status.	24
2.6	User interface: allocation.	25
2.7	User interface: the optimal schedule of the household.	26
2.8	User interface: performance of the HVAC for the household.	26
2.9	User interface: overall review of energy storages.	27
2.10	User interface: detailed schedule of single energy storage.	28
3.1	Daily charts for the parameters in Ennis.	33
3.2	Region map and households' locations in Ennis, Ireland.	34
3.3	Operational cost reduction varying the ownership rate of PV system and PES in Ennis.	36
3.4	Features for charging and discharging of PES.	37
3.5	Operational cost varying battery capacity and number of CES.	40

3.6	Operational cost for different CES allocation options.	42
3.7	Comparing battery charging, discharging, state of charge, and ratio of charging vs discharging among different CES allocation options in summer: [R] CES-random [D] CES-diverse [H] CES-homogeneous.	43
3.8	Comparing the households' load in each period and total households' load connected to the same CES for different CES allocation options in summer: [R] CES-random [D] CES-diverse [H] CES-homogeneous.	44
3.9	Comparing per household utilization rate of the energy storage among different allocation options in the summer day: [R] CES-random [D] CES-diverse [H] CES-homogeneous [P] PES-single.	45
3.10	Comparing charging and discharging times of households among different allocation options in the summer day: [R] CES-random [D] CES-diverse [H] CES-homogeneous [P] PES-single.	46
3.11	Comparing overall utilization rate of CESs among different CES allocation options in the summer day: [R] CES-random [D] CES-diverse [H] CES-homogeneous.	47
3.12	Fairness comparison for different CES allocation options in the summer day: [R] CES-random [D] CES-diverse [H] CES-homogeneous.	49
3.13	Daily charts for the parameters in Waterloo.	51
3.14	Region map and households' locations in Waterloo, Canada.	54
3.15	Operational cost reduction varying the ownership rate of PV system and PES in Waterloo.	55
3.16	Features for charging and discharging of PES.	56
3.17	Operational cost varying battery capacity and number of CES.	57
3.18	Operational cost for different CES allocation options.	58
3.19	Comparing battery charging, discharging, state of charge, and ratio of charging vs discharging among different CES allocation options in summer: [R] CES-random [D] CES-diverse [H] CES-homogeneous.	59
3.20	Comparing the households' load in each period and total households' load connected to the same CES for different CES allocation options in summer: [R] CES-random [D] CES-diverse [H] CES-homogeneous.	60

3.21	Comparing per household utilization rate of the energy storage among different allocation options in the summer day: [R] CES-random [D] CES-diverse [H] CES-homogeneous [P] PES-single.	61
3.22	Comparing charging and discharging time of households among different allocation options in the summer day: [R] CES-random [D] CES-diverse [H] CES-homogeneous [P] PES-single.	62
3.23	Comparing overall utilization rate of CESs among different CES allocation options in the summer day: [R] CES-random [D] CES-diverse [H] CES-homogeneous.	63
3.24	Fairness comparison for CES allocation options in the summer day: [R] CES-random [D] CES-diverse [H] CES-homogeneous.	64

List of Tables

3.1	Ownership rates of home appliances in Ennis, Ireland	30
3.2	Parameters of home appliances in Ennis, Ireland	31
3.3	Average battery capacity for each household in Ennis	39
3.4	The capital costs of CES combinations	41
3.5	Parameters of home appliances in Waterloo, Canada	52
3.6	Ownership rates of home appliances in Waterloo, Canada	53

List of Symbols

Sign	Description	Unit
T	time horizon that devices and energy storages are scheduled	
ΔT	duration of each time step	h
Π_t	price of electricity at time t	\$/kWh
A^{\max}	maximum power capacity limitation of aggregator	kW
A^{\min}	minimum power capacity limitation of aggregator	kW
A_t	aggregated load on the aggregator at time t	kW
R	set of households	
H_r^{\max}	maximum power capacity limitation of household r	kW
H_r^{\min}	minimum power capacity limitation of household r	kW
$H_{r,t}$	household r net load at time t	kW
$D_{r,t}$	actual demand from home appliances of household r at time t	kW
D_r	set of devices which household r contains	
$\tilde{C}_{d,t}$	power generation of photovoltaic system d at time t	kW
$C_{d,t}^{avg}$	initial data for power generation of photovoltaic system d at time t	kW
$\tilde{U}_{d,t}$	power consumption of provincial load d at time t	kW
$U_{d,t}^{avg}$	initial data for power consumption of provincial load d at time t	kW
$\tilde{I}_{d,t}$	power consumption of uninterruptable load d at time t	kW
$i_{d,t}$	binary status indices of uninterruptable load d at time t	
L	single cycle of duration of uninterruptable load	
$\theta_{d,t}^c$	power consumption of of thermal load d on cooling mode at time t	kW
$\theta_{d,t}^h$	power consumption of of thermal load d on heating mode at time t	kW
θ_d^{\max}	maximum power capacity limitation of thermal load d	kW
θ_d^{\min}	minimum power capacity limitation of thermal load d	kW
$\Theta_{d,t}$	indoor temperature of thermal load d at time t	°C
$\Theta_{d,t}^{amb}$	ambient temperature of thermal load d at time t	°C
$\Theta_{d,t}^m$	temperature modification from thermal load d at time t	°C

Sign	Description	Unit
Θ_d^{set}	setting temperature by thermal load d at time t	$^{\circ}\text{C}$
$\Theta_{d,t}^{avg}$	initial data for ambient temperature of thermal load d at time t	$^{\circ}\text{C}$
γ	degrees tolerance of thermal load d	$^{\circ}\text{C}$
C_d	thermal capacitance of thermal load d	$\text{kWh}/^{\circ}\text{C}$
R_d	thermal resistance of thermal load d	$^{\circ}\text{C}/\text{kW}$
η_d	working efficiency factor of thermal load d	
$t_{d,t}^c$	binary status indices of thermal load d on cooling mode at time t	
$t_{d,t}^h$	binary status indices of thermal load d on heating mode at time t	
E	set of energy storages	
E_r	set of energy storages which household r connects	
R_e	set of households which each energy storage e serves	
$S_e^{ch. max}$	maximum charging power limitation of energy storage e	kW
$S_e^{ch. min}$	minimum charging power limitation of energy storage e	kW
$S_e^{dis. max}$	maximum discharging power limitation of energy storage e	kW
$S_e^{dis. min}$	minimum discharging power limitation of energy storage e	kW
$S_{r,e}^{ch. max}$	maximum charging power limitation of household r to CES e	kW
$S_{r,e}^{ch. min}$	minimum charging power limitation of household r to CES e	kW
$S_{r,e}^{dis. max}$	maximum discharging power limitation of household r to CES e	kW
$S_{r,e}^{dis. min}$	minimum discharging power limitation of household r to CES e	kW
$S_{e,t}^{ch}$	charging power consumption of energy storage e at time t	kW
$S_{e,t}^{dis}$	discharging power consumption of energy storage e at time t	kW
$S_{r,e,t}^{ch}$	charging power consumption of energy storage e from household r at time t	kW
$S_{r,e,t}^{dis}$	discharging power consumption of energy storage e from household r at time t	kW
B_e^{max}	maximum battery state of charge of energy storage e	kWh
B_e^{min}	minimum battery state of charge of energy storage e	kWh
$B_{e,t}$	battery state of charge of energy storage e at time t	kWh
η_e^{ch}	charging efficiency of energy storage e	$\%$
η_e^{dis}	discharging efficiency of energy storage e	$\%$
$s_{r,e,t}^{ch}$	binary status indices of energy storage e on charging mode from household r at time t	
$s_{r,e,t}^{dis}$	binary status indices of energy storage e on discharging mode from household r at time t	

Chapter 1

Introduction

This chapter introduces the motivation of this research, related research in the domain of Home Energy Management System (HEMS) and Distributed Energy Resources (DERs) for a single household and for communities, especially in the field of Energy Storage System (ESS). Additionally, the objective and the structure of this thesis are introduced.

1.1 Motivation

Global energy demand has continued to rise since the mid-20th century as a result of industrial development and population growth. According to the historical record in Ontario, Canada, electricity consumption increased by almost 250% from 1962 to 1990 [1] and fluctuated between 140 and 160 terawatt hours from 1990 to 2018 [1] [2] as seen in Figure 1.1. Additionally, high industrial and residential growth caused grid stations to be at high capacity [3], especially in cities such as Toronto and Ottawa which lead to potential risks of power supply, such as power outage by overcapacity in a particular area. As a result, it is challenging for the transmission system operators to provide reliable power to consumers.

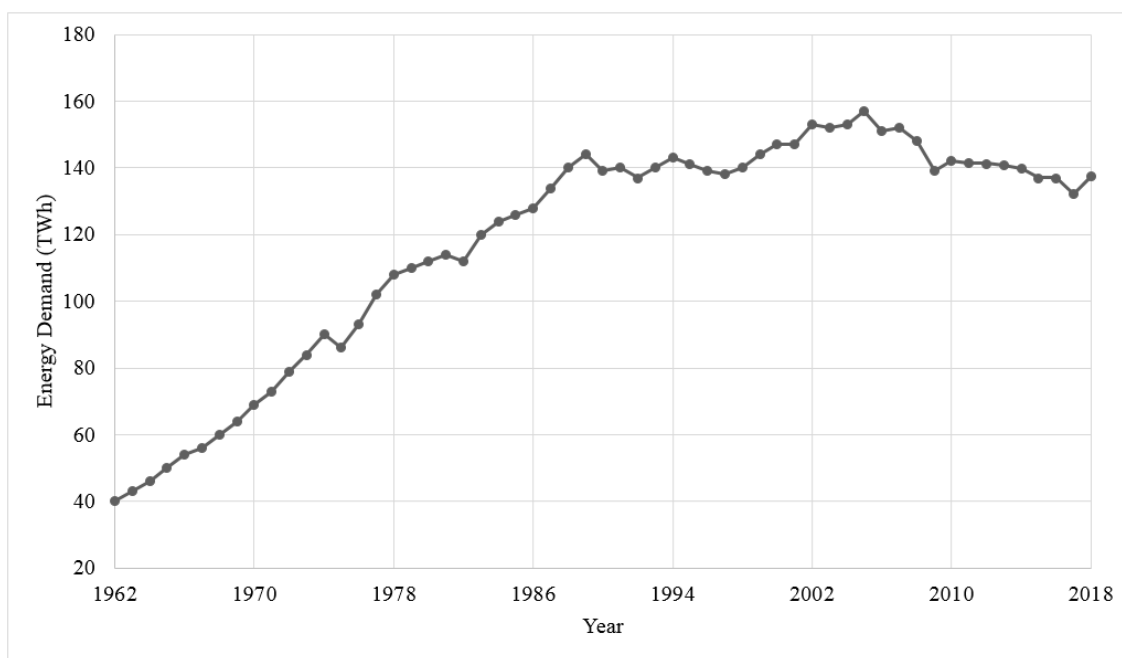


Figure 1.1: Electricity consumption in Ontario, Canada between 1962 and 2018.

Source: [1], [2]

Reacting to the strong growth in electricity consumption, power systems are undergoing a fundamental transition due to the emergence of renewable, distributed and flexible energy resources that can actively manage consumers' consumption, production and storage of energy. The development of distributed energy sources has become a matter of priority

to keep up with increasing demand and to limit greenhouse gas emissions. However, the widespread adoption of renewable energy has been limited by its drawbacks, namely, the variability and intermittency of generation that can lead to demand-supply imbalances and challenges to grid operation. A key strategy to overcome such issues is the implementation of improved intelligence and flexibility in the distribution network. In particular, smart grids increase the electric energy efficiency by meeting the dynamic demand responses, reducing the power loss from generation to consumption through energy storage, utilizing new supplies of renewable green energy, including wind and solar, and the ever-increasing use of microgrid, electric vehicles (EVs) and smart appliances.

Recently, the work presented in [4] has surveyed the field of smart grid and systematically reviewed recent literature. In a smart grid setup, households cooperate with aggregators to help shape the successful operation of a more reliable power system and receive some benefits from aggregators, such as value-added services and better energy management. Though the authors indicate that the area of collaboration in energy management system correspond to one of the most "popular" topics in the field of smart grid, little research has been done under the concept of "sharing energy", especially in the field of ESS. Thus, this research takes the concept of community into account and aims to develop a framework to share resources in a realistic community environment.

1.2 HEMS and DERs for a Single Household

Households can potentially play an important role in the demand side management of energy services as a part of smart grid. They can control their smart appliances and share information regarding their power consumption through a HEMS while using DERs to adjust their electricity consumption [5]. For example, when households install DERs, such as rooftop photovoltaic panels, to generate electricity for their daily power demand, over-production of electricity can be controlled by the HEMS to allow the household to have flexibility to store surplus power via the energy storages [6] or participate in local energy markets which are introduced by the aggregator through smart grid communication [7] to achieve economic efficiency. Thus, households would benefit from the smart grid technology by taking control of their daily electric energy consumption more effectively, saving money, and help protect the environment. Figure 1.2 shows common DERs and a HEMS in a typical household.

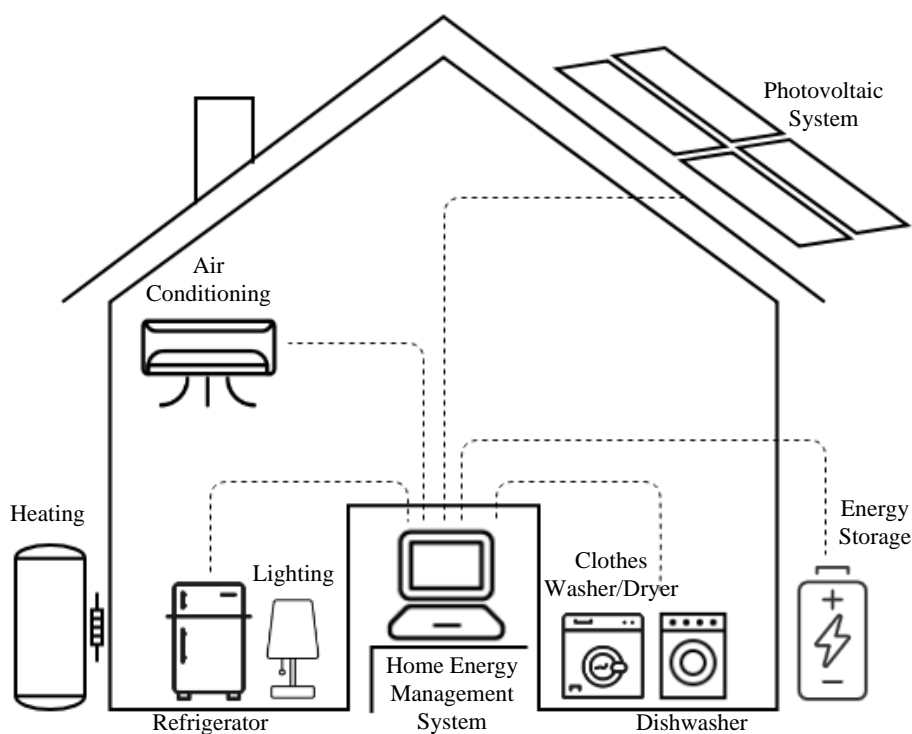


Figure 1.2: HEMS and DERs in a single household.

Recent research describes various models to optimize the coordination of DERs and HEMS for households, which includes different constraints to take into account various types of electric loads. First, HEMS is considered for a single household to improve its energy efficiency. In [8], the authors present mathematical optimization models of residential energy hubs in smart grids, which optimally control all major residential energy loads, storage and production components, including fridge, freezer, dishwasher, washer and dryer, stove, water heater, hot tub, and pool pumps. After applying the proposed model to a real household in Ontario, Canada, the results show that the household saves on energy costs and peak demand while maintaining the household owner’s desired comfort levels. Also, the work of [9] focuses on peak load reduction in commercial buildings and industrial facilities. The methods are presented using 15-minute-interval electric load data in California to help building managers understand building energy consumption. The author investigates methods to coordinate aggregations of residential thermostatically controlled loads (TCLs), including air conditioners and refrigerators, to manage frequency and energy imbalances in power systems. Based on demand response (DR) paradigms, Markov Chain models are developed to describe the temperature state evolution of heterogeneous populations of TCLs and Kalman filtering is used for estimation.

In addition to mathematical optimization models, different approaches are used to solve such problems. For example, the work in [10] evaluates the performance of heuristic algorithms: Genetic Algorithm and Artificial Fish Swarm Algorithm to optimally schedule appliances in a household. Also, in [11] the authors propose a long short-term memory-based deep-learning forecasting framework with appliance consumption sequences to address the schedules. The work in [12] develops a real time optimal schedule controller for HEMS using a new Binary Backtracking Search Algorithm to effectively manage the energy consumption.

DERs are also taken into account for a household to take the daily electricity consumption more effectively. In [13], the authors propose a detailed HEMS structure, which considers hourly pricing and peak power limiting, to determine the optimal day-ahead appliance scheduling of a smart-household based DR strategies. All types of controllable appliances and DERs have been explicitly modeled, which include water heater, air conditioner, washing machine and dishwasher, EVs, ESS, and distributed generation at the end-user premises. Moreover, [14] presents a mathematical model for the optimal energy management of a residential building and proposes a centralized energy management system (CEMS) framework for off-grid operation with energy production facilities, e.g., solar rooftops and batteries. Energy production facilities which in conjunction with smart meters can function as smart energy hubs coordinating the loads and the resources in an optimal manner, and the model of each component of the hub is integrated within the

CEMS. From the models, the optimal decisions are determined in real-time with realistic parameter settings and customer preferences. Finally, the battery size of ESS is considered. In [15], the authors formulate a model to determine optimal energy and power capacity of a stationary battery storage in order to minimize electricity payments. Robust and stochastic optimization for individual building are introduced, and these models are compared on a real-world load data of a hotel in Croatia.

Consequently, the presented literature successfully analyzes individual household's behaviors, and provides short term optimal operation schedules for households under different scenarios. However, it does not take into account the community as a whole. Thus the solution presented although optimal at the individual household level, it may not be optimal at the community level.

1.3 Community in Smart Grid

1.3.1 The Concept of a Community

The concept of a community has been seen in recent studies, which group multiple households together that are located in a particular area and interact with each other. Recent studies start to analyze potential economical benefits based on the dispatch of residential loads and distributed generation of households in a small community or an apartment, such as optimal energy purchase price, an optimal schedule for certain period, etc.

The work presented in [16], [17], [18] describes various models considering the community as a whole to optimize households' demand. First, the work of [16] proposes an energy scheduling and distributed storage (ESDS) algorithm to minimize consumer energy expenditure and maximize demand satisfaction simultaneously. After testing energy consumption data of hundred flats, the ESDS algorithm was found to offer consumer-friendly and utility-friendly enhancements. Moreover, in [17] the paper presents a DR scheduling model by formulating a mixed integer linear programming (MILP) for the novel residential community incorporating the current circumstances and the future trends of DR programs. By testing on a real case in China, the presented model reduces the energy purchase cost of user's electricity consumption and decreases the peak load and peak-valley difference of residential load. Furthermore, in [18] the authors propose a decentralized methodology for optimal coordination of DERs, which calculates the energy purchase price of multiple households. The proposed approach is based on Dantzig-Wolfe decomposition and column generation, thus it allows to integrate any type of resource whose operation can be formulated within an MILP. Finally, regarding battery size of ESS, related studies consider a large, independent range, such as isolated microgrid [19], to analyze the optimal battery capacity [20].

In summary, the models above consider large-scale instances covering a whole community, however, their analysis is still at the individual household level without considering the option of sharing these resources among the households as a community.

1.3.2 Sharing in a Community: Community Energy Storage

In contrast to individual energy storage, the field of Community Energy Storage (CES) is now gaining more attention in various countries. The advantages of CES are significant as they are easy to install and maintain, provide a better fit into smart grid, and can reduce power loss and energy cost [21] [22].

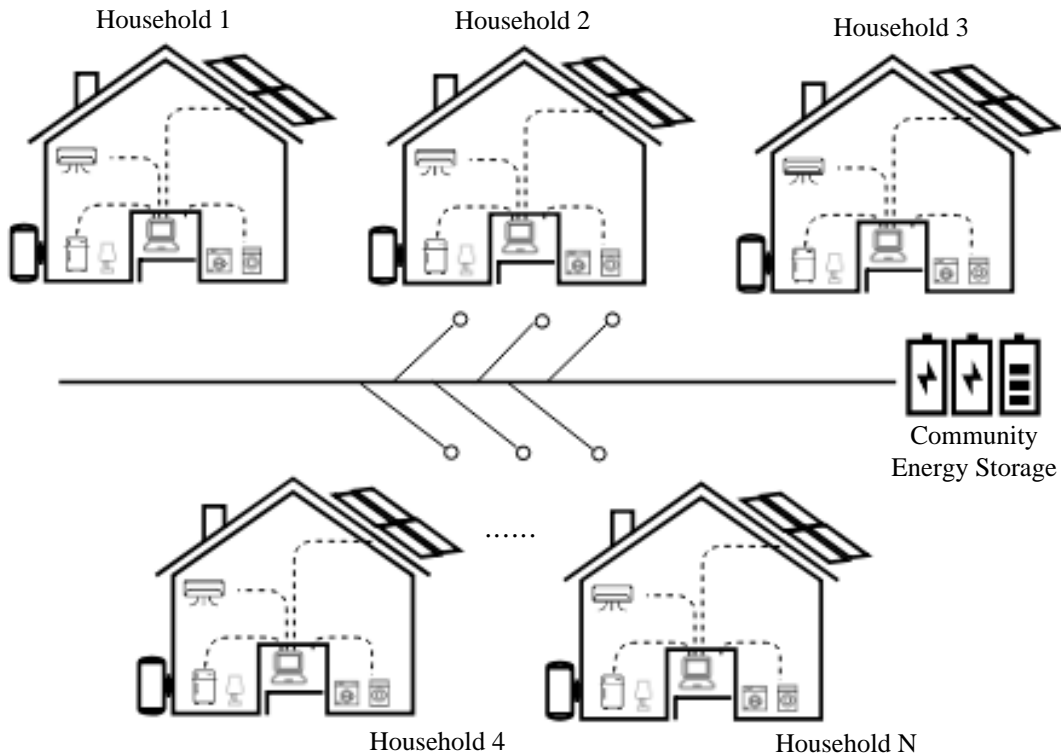


Figure 1.3: Schematic diagram of CES in a community.

Recently, related work focused on the relationship of the community size, CES, and DERs with electricity generation (e.g., Photovoltaic (PV), wind generation). First, in [23] the authors propose an approach based on center of gravity theory to determine the location of CES for minimizing the annual energy loss. Also, they identified a proper rated capacity of CES and its hourly dispatch strategy for achieving a desired annual load factor, flattening the daily demand profile, and improving the voltage profile by the daily demand profile and PV generation of a community. From the same authors, the work of [24] proposes a strategy for optimal allocation of multiple CES units in a distribution system with PV generation. It considers all possible benefits, e.g. energy arbitrage, peak power generation, and energy loss reduction. It also includes an optimal power factor approach to dispatch CES units to improve load factors and voltage profiles.

Additionally, in [25] the authors calculate the optimal performance of CES, including the round trip efficiency and annual discharge, levelized cost of electricity, and the internal rate of return by performing PV energy time-shift and using real demand data given

different sizes of the community. Also, [26] formulates a stochastic constrained problem based on the Lyapunov optimization theory to minimize the overall cost of the community, including the cost of purchasing electricity from the main grid, and the cost of charging and discharging ESSs. Moreover, the approach in [27], uses the k -means method to categorize customers by their electricity consumption patterns, and find the optimal capacity of different DERs by formulating a linear programming optimization model and presenting the concept of Peer-to-peer (P2P) energy trading. The presented work provides several economic benefits to communities, such as maximizing the local demand and supply balancing, facilitating a P2P energy trading market paradigm, and providing guidelines of appropriate shares of DERs for better constructing future networks.

Considering the studies of CES above, households in their community can be more efficient in consuming and generating electricity. However, there is still room for improvement. One direction is to consider the fairness and economic feasibility of sharing energy storage. Related approaches, e.g., multi-agent based models [28] [29], auction-based [30], cooperative game-theoretic approach [31], are proposed to optimize energy consumption, allocation, and management of ESSs for a smart grid.

The other research direction is focused on battery size of CES to reduce installation and operational costs. For instance, [32] presents the CES at the community level which groups them into communities of neighbors using real locations and road network. The authors consider PV generation and installation costs to determine the optimum storage size. In [33], the authors compare the technical and economic feasibility of single private energy storage and CES with PV generation by formulating the problem as an MILP with the objective of minimizing the costs of power received from the grid. Similarly, [34] considers a sharing-based ESS architecture for any network size with an arbitrary number of customers to find the optimal CES size. Finally, [35] proposes a multi-stage stochastic program model to minimize community electricity purchase cost to support a new energy management framework and obtain a suitable size of CES and distributed PV generation. Therefore, for the optimal battery size of CES and various allocation options, households have better ways to optimize their energy costs.

1.4 Thesis Objective

From the studies presented in the previous section, the model formulation of integrating energy storage has been developed widely, however, some features remain missing to make the models less realistic, such as physical limitation of the energy storage systems, different allocation options, fairness, etc. Therefore, the objective of this thesis are as follows:

- Develop a framework for effective allocations of CES using machine learning by considering different physical limitation, including geographical locations of households, number of devices, equipment specifications, etc.
- Optimize households' operations in a community systemically by considering various types of appliances, DERs, and various operating conditions, such as summer and winter.
- Present a software with a user interface which can be applied to general real cases given appropriate input data.
- Analyze the computational results using two use-cases to evaluate the deployment of shared energy storage.

This research develops a framework for effective allocations, utilization of CES, and optimization of its operations. Machine learning methodology is used for allocating the CES to different households given different battery size and number, and an MILP model is presented to optimize the energy costs while satisfying household demand operations for a community in a smart grid. To show the performance of the proposed approaches, two real use cases are considered: Waterloo, Canada and Ennis, Ireland. The testing is done on two typical days, one in the winter and one in the summer. Finally, the computational results are presented graphically to show the advantage of using CES as opposed to PES.

The thesis is divided into four chapters. Chapter 2 describes the solution methodology, including setting up a community based on machine learning methodology, allocating energy storage to households based on several criteria, and optimizing the operational cost via an MILP model. The software with the user interface is also introduced in this chapter. Chapter 3 simulates two real cases, which are Waterloo, Canada and Ennis, Ireland, and presents computational results to compare different allocation options of energy storage and their impact on costs and other KPIs. Chapter 4 highlights the conclusion and discusses future research directions.

Chapter 2

Solution Methodology

The proposed research aims to minimize the operational cost of electricity considering various load options of appliances and PV and energy storage set-ups. The operation scheduling for households is optimized given different allocation options of the energy storage from private energy storage to community energy storage. The approach proposed includes three parts: community setting, allocation options for energy storages, and operational cost optimization. The process flow of the solution approach is presented in [Figure 2.1](#).

First, the community is set-up by considering the physical limitation of the network, for example, households cannot connect to energy storage devices exceeding a given geographical distance. Additionally, for setting-up the community, the number of home appliances and the number of PVs for the households are estimated depending on the historical data. The second step is related to the allocation options for energy storage devices. In this work, we consider four options to the households, including the option of PES and three options of CES: random, diverse, and homogeneous allocation. Finally, the third step is to optimize the operations of the energy storages and the households to obtain the minimum electricity cost for the aggregator based on the various settings.

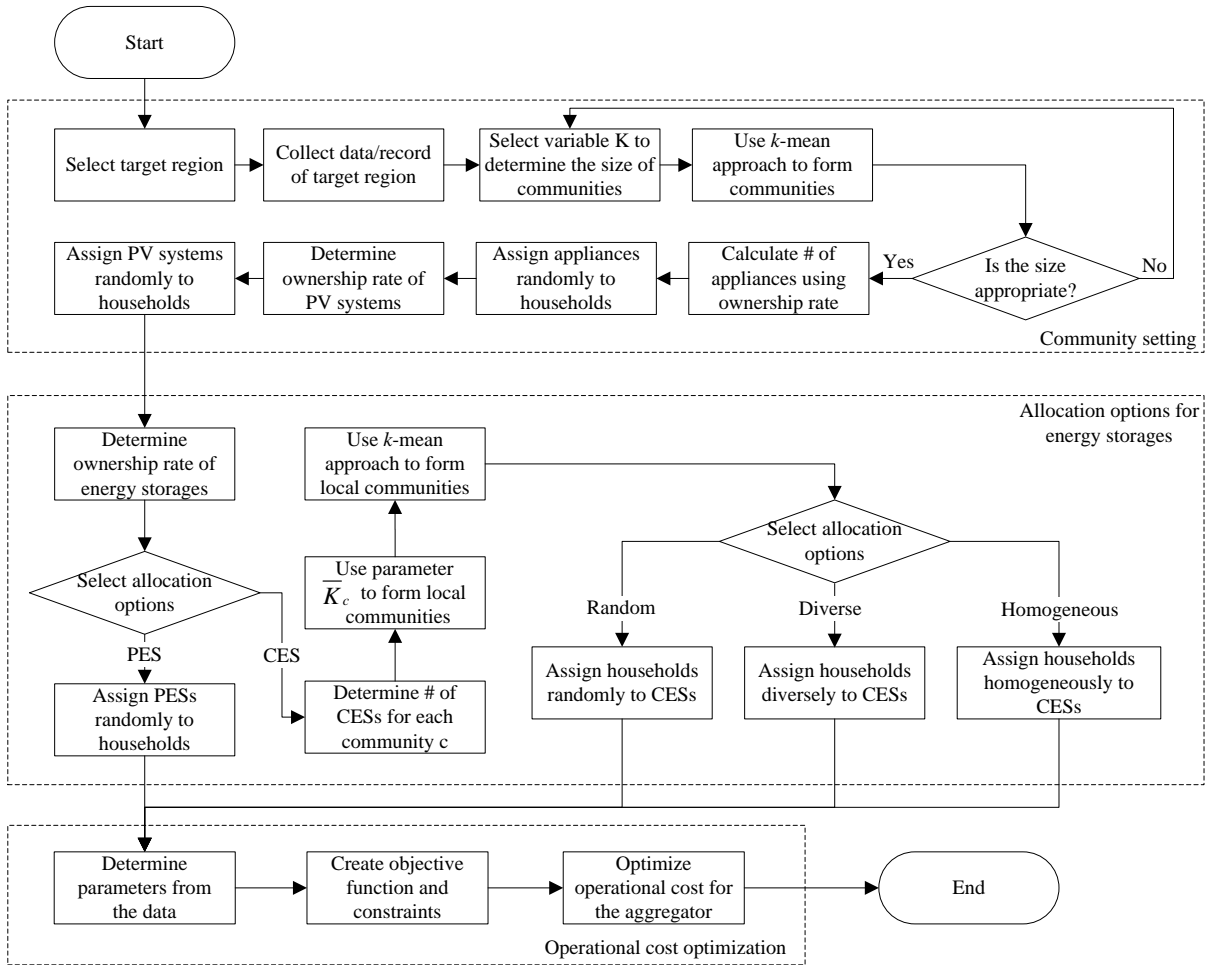


Figure 2.1: Flow chart of the solution approach.

2.1 Community Setting

The first step in the proposed approach is to consider a given region to apply the various allocation options. All the data is collected based on the features of the households in the given region, including its geographical location, temperature history, specifications of devices, ownership rate of devices, and record of power consumption and generation, etc. After gathering the data, the region is separated into communities based on households' geographical locations by using k -mean approach. In this research, the communities are defined by the distribution limitation of CES, such as the layout of electric power transmission, the distance of distribution circuits, and the capacity of power rating, etc. The k -means approach works iteratively to determine the K groups of the households using the following equation:

$$J = \sum_{j=1}^K \sum_{i=1}^n (x_i^j - c_j)^2 \quad (2.1)$$

The objective function (2.1) is to minimize the distance between the data point x_i , that represents the GPS coordinates of a given household i , to the centroid for cluster j , c_j , to allocate the data points to K groups. The data points are clustered based on feature similarity, and the feature for communities is their geographical location. From objective function (2.1), x_i^j is the i -th household's geographical location which has been assigned to the j -th cluster with centroid location c_j . To present the reality, the variable K would be selected based on the size of the region and to meet the physical limitations of the system. Household's location is formed based on its corresponding address from Open Street Maps and the household's connection to the energy storage is assumed to follow the public roads instead of crossing the private properties.

Additionally, the number of home appliances, including provincial load, uninterruptible load, and thermal load, are determined by the ownership rate of devices for the households. The ownership rate is collected from official data sources related to the region. Based on the ownership rate, these devices are assigned randomly to the households. For example, if the ownership rate of dish washer is 60% and there are 100 households, 60 dish washers are formed and would be assigned randomly to these households. Similarly, the number of PV systems and the number of PES are created by the ownership rate; the ownership rate for various loads as well as the PV systems and the energy storage devices are varied to study various scenarios.

2.2 Allocating Energy Storage Systems

After the community set-up phase, the approach allocates the energy storage devices to the households and forms local communities. Four allocation options for the local communities are considered: private energy storage (PES-single), community energy storage with random allocation (CES-random), community energy storage with diverse allocation (CES-diverse), and community energy storage with homogeneous allocation (CES-homogeneous).

The PES-single option is assumed when households have their own energy storage, which is independent from other households. The other three options CES-random, CES-diverse, and CES-homogeneous assume that several households in the local community share a given CES. For the CES, households are clustered again using k -mean approach (2.1), the clusters are determined based on the power consumptions of households, which includes the provincial load. The number of groups in this case is \bar{K}_c and it is chosen based on the number of CES desired for each community c .

After the \bar{K} clusters are determined, the households in the clusters are assigned to CESs based on the allocation options, which are displayed in Figure 2.2. One assumption is that all the CESs in one community are assigned to almost the same number of households. For example, if there are 21 households with 5 CESs, CESs would be assigned 5, 4, 4, 4 and 4 households, respectively. Additionally, the proposed approach assumes that the household would have higher motivation to install the energy storage when it has the PV system, and vice versa.

When households are allocated to CESs, there are three allocation options which are considered. CES-random states that households from the same cluster are assigned randomly to any of the CES which the community has. CES-diverse implies that the households from the same cluster would be assigned uniformly to different CESs. As a result, CESs will have households with different power consumption profiles. CES-homogeneous states that the households from the same cluster would be assigned to one CES and hence households with similar power consumption profile are assigned to the same CES. CES-diverse and CES-homogeneous represent two extreme allocation scenarios and CES-random is similar to the reality as the consumption profiles of the households might not be known in advance.

In summary, Figure 2.3 provides a simple example that shows how the households are allocated in a selected region. In this example, the selected target regions are separated by using k -mean approach into three communities, i.e., $K = 3$. Then, given a total of seven CESs in this region, the households are grouped by $\bar{K}_1 = 3$, $\bar{K}_2 = 2$, and $\bar{K}_3 = 2$,

respectively. Based on the groups, the households are allocated to CESs based on the selected allocation option.

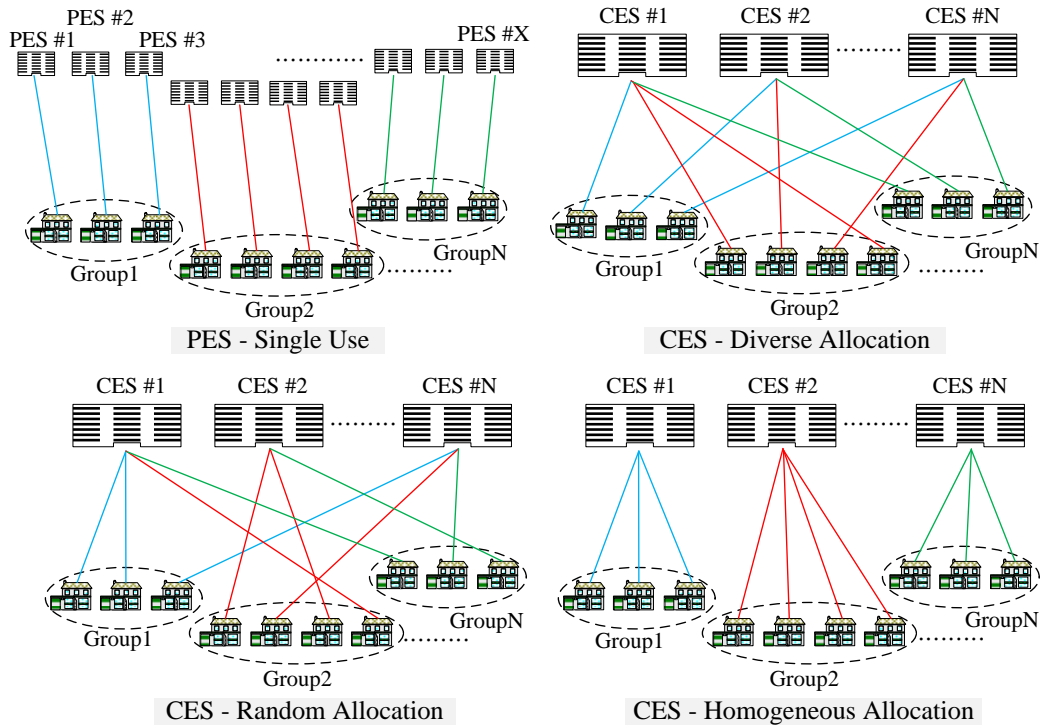


Figure 2.2: Different allocation options of the CES.

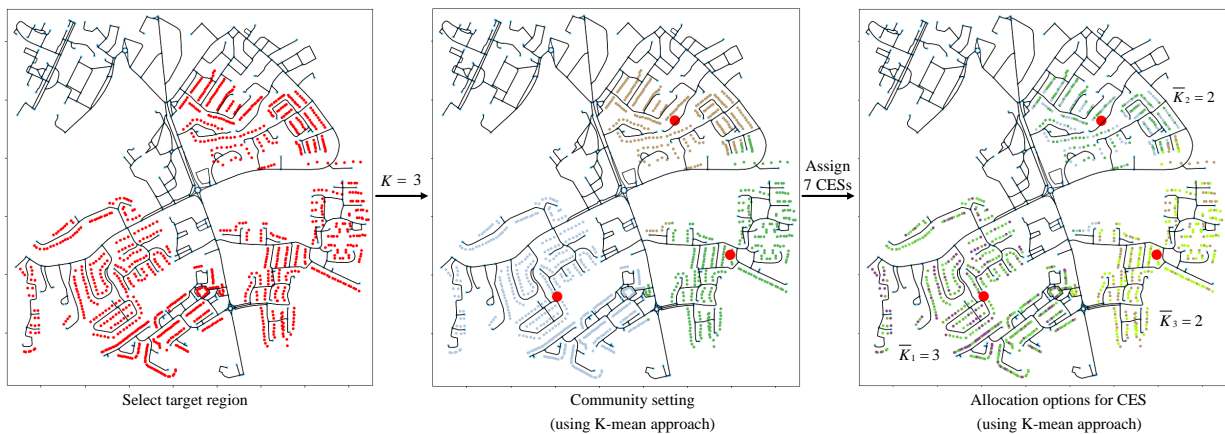


Figure 2.3: An example for forming communities and allocations for CESs.

2.3 Operational Cost Optimization

The third and last step is to have the optimization model to optimize the operations of the whole system. In this formulation, the time horizon is considered to be 24 hours where $T = \{0, \dots, 23\}$ with a time step, Δ_T , of one hour. The mathematical formulation is given below.

$$\min \sum_{t \in T} \Pi_t \Delta_T A_t \quad (2.2)$$

The objective function (2.2) is to minimize the total cost of purchasing energy from the grid, while satisfying all operational constraints. The basic assumption is that there is only one aggregator serving the grid and the objective minimizes the cost of the aggregator.

$$A^{\min} \leq A_t \leq A^{\max} \quad \forall t \in T \quad (2.3)$$

$$A_t = \sum_{r \in R} H_{r,t} \quad \forall t \in T \quad (2.4)$$

For the aggregator, constraint (2.3) indicates that the aggregator must ensure that the aggregated load A_t is within the range of the physical limitations. Constraint (2.4) states the relationship between the households' net load and the aggregated load at time t . For each household's net load $H_{r,t}$, the constraints are listed as below:

$$H_r^{\min} \leq H_{r,t} \leq H_r^{\max} \quad \forall t \in T \quad (2.5)$$

$$H_{r,t} = D_{r,t} - \sum_{d \in D_r} \tilde{C}_{d,t} + \sum_{e \in E_r} (S_{r,e,t}^{ch} - S_{r,e,t}^{dis}) \quad \forall t \in T \quad (2.6)$$

Similarly, constraint (2.5) indicates the physical limitation of household's net load. For each household, constraint (2.6) states the relationship between the household's net load and the algebraic power from appliances installed in the household. In constraint (2.6), $D_{r,t}$ represents the summation of power consumptions from different types of home appliances. Also, the power generation from the PV system $\tilde{C}_{d,t}$ and the net load coming from the energy storage connected to that household is included. The PV system generates power for the household and assumes that all power is only used by the household and does not export to the grid.

Moreover, considering home appliances for a household, $D_{r,t}$ is formed as constraint (2.7), including provincial load, uninterruptable load, and thermal load. The constraint is

shown as below:

$$D_{r,t} = \sum_{d \in D_r} \tilde{U}_{d,t} + \sum_{d \in D_r} \sum_{k=0}^{L-1} i_{d,t-k} \tilde{I}_{d,k} + \sum_{d \in D_r} (\theta_{d,t}^c + \theta_{d,t}^h) \quad \forall t \in T \quad (2.7)$$

The provincial load $\tilde{U}_{d,t}$ includes the home appliances which are necessary for daily use and cannot be controlled, e.g., refrigerator, lighting, etc. Then, the constraints of uninterruptible load are formulated:

$$\sum_{t=0}^{|T|-1} i_{d,t} = 1 \quad \forall t \in T \quad (2.8)$$

$$i_{d,t} \in \{0, 1\} \quad (2.9)$$

The uninterruptible loads define the home appliances which the household owner can turn on the devices in a specific period, and cannot be interrupted until the operations finish, in other words, it has its single cycle of duration L , e.g., dish washer, clothes washer, clothes dryer, etc. For each appliance, it has its power consumptions in its cycle at time k , which means $\tilde{I}_{d,k}$, and it is received by the specification of appliance from the case. Constraints (2.8), (2.9) describe the status of uninterruptible load at time t , constraints (2.8) define that each appliance can be opened once during period T . Additionally, the cycle of the appliance is assumed to operate completely once it is triggered. The constraints for thermal load are displayed as follows:

$$\Theta_{d,t+1} = a_d \Theta_{d,t} + (1 - a_d)(\Theta_{d,t}^{amb} - \Theta_{d,t}^m) \quad \forall t \in T \quad (2.10)$$

$$a_d = e^{-\Delta T / c_d R_d} \quad (2.11)$$

$$\Theta_{d,t}^m = R_d \eta_d (\theta_{d,t}^c - \theta_{d,t}^h) \quad \forall t \in T \quad (2.12)$$

$$t_{d,t}^c \theta_d^{\min} \leq \theta_{d,t}^c \leq t_{d,t}^c \theta_d^{\max} \quad \forall t \in T \quad (2.13)$$

$$t_{d,t}^h \theta_d^{\min} \leq \theta_{d,t}^h \leq t_{d,t}^h \theta_d^{\max} \quad \forall t \in T \quad (2.14)$$

$$t_{d,t}^c + t_{d,t}^h \leq 1 \quad \forall t \in T \quad (2.15)$$

$$t_{d,t}^c, t_{d,t}^h \in \{0, 1\} \quad (2.16)$$

$$\Theta_d^{set} - \gamma \leq \Theta_{d,t} \leq \Theta_d^{set} + \gamma \quad \forall t \in T \quad (2.17)$$

$$\Theta_{d,T} = \Theta_d^{set} \quad (2.18)$$

The thermal load includes heating, ventilation, and air conditioning (HVAC) which controls the indoor temperature of the household. It is normally formed as constraints (2.10)

to (2.18). Constraint (2.10) shows the indoor temperature of next time step is influenced by the current indoor temperature, ambient temperature, and modified temperature from HVAC. a_d is the parameter defined from thermal capacitance C_d and thermal resistance R_d (2.11). When HVAC adjusts the temperature, it has its working efficiency factor η_d , and it can control the temperature based on cooling mode or heating mode at time t (2.12). Constraints (2.13)-(2.16) show that HVAC can open either cooling mode or heating mode at time t corresponding its power consumption $\theta_{d,t}^c$ or $\theta_{d,t}^h$. Moreover, the indoor temperature has the range which allows γ degrees tolerance compared to the setting temperature by HVAC (2.17). Finally, constraint (2.18) assumes that the final indoor temperature after calculation should be equal to the setting temperature.

Energy storages are used to store power generated by PV systems or adjust households' power consumption. The constraints of energy storage consider both types: PES and CES, which are shown as below:

$$B_e^{\min} \leq B_{e,t} \leq B_e^{\max} \quad \forall t \in T \quad (2.19)$$

$$S_{e,t}^{ch} = \sum_{r \in R_e} S_{r,e,t}^{ch} \quad \forall t \in T \quad (2.20)$$

$$S_{e,t}^{dis} = \sum_{r \in R_e} S_{r,e,t}^{dis} \quad \forall t \in T \quad (2.21)$$

Constraint (2.19) indicates that the battery state of charge must be within the range of physical limitations. Constraint (2.20) states that the overall charging power is modeled as the summation of the charging power by the set of households connected to storage e . Similarly, the overall discharging power is modeled, see constraint (2.21).

$$\Delta_T(\eta^{ch} S_{e,t}^{ch} - \frac{1}{\eta^{dis}} S_{e,t}^{dis}) = B_{e,t} - B_{e,t-1} \quad \forall t \in T \quad (2.22)$$

$$S_e^{ch.\min} \leq S_{e,t}^{ch} \leq S_e^{ch.\max} \quad \forall t \in T \quad (2.23)$$

$$S_e^{dis.\min} \leq S_{e,t}^{dis} \leq S_e^{dis.\max} \quad \forall t \in T \quad (2.24)$$

$$s_{r,e,t}^{ch} S_e^{ch.\min} \leq S_{r,e,t}^{ch} \leq s_{r,e,t}^{ch} S_e^{ch.\max} \quad \forall r \in R_e, \forall t \in T \quad (2.25)$$

$$s_{r,e,t}^{dis} S_e^{dis.\min} \leq S_{r,e,t}^{dis} \leq s_{r,e,t}^{dis} S_e^{dis.\max} \quad \forall r \in R_e, \forall t \in T \quad (2.26)$$

$$s_{r,e,t}^{ch} + s_{r,e,t}^{dis} \leq 1 \quad \forall r \in R_e, \forall t \in T \quad (2.27)$$

$$s_{r,e,t}^{ch}, s_{r,e,t}^{dis} \in \{0, 1\} \quad (2.28)$$

Additionally, the battery efficiency is considered. Constraint (2.22) states the internal dynamic of the battery at a given time step t . The parameters η^{ch} and η^{dis} are the transfer

efficiency of battery when the energy storage is charging and discharging, respectively. Constraint (2.23) and (2.24) model the charging power and discharging power from the energy storage e which cannot exceed the maximum electric power capacity at time t . Additionally, constraint (2.25)-(2.28) indicate that the energy storage cannot be charge and discharge simultaneously from a given household r given time t . If several households link to a CES, then $S_e^{ch.\min}$, $S_e^{ch.\max}$, $S_e^{dis.\min}$, $S_e^{dis.\max}$ in constraints (2.25) and (2.26) are replaced by $S_{r,e}^{ch.\min}$, $S_{r,e}^{ch.\max}$, $S_{r,e}^{dis.\min}$, $S_{r,e}^{dis.\max}$, respectively.

Finally, the data sometimes only provides an average amount for a given region without any information on the performance of the individual devices of the households. In this case, an estimate of the load of certain devices is used as follows:

$$\tilde{C}_{d,t} = \rho_{d,t}^c C_{d,t}^{avg} + 0.01 \varepsilon_{d,t}^c \quad \forall t \in T \quad (2.29)$$

$$\tilde{U}_{d,t} = \rho_{d,t}^h (U_{d,t}^{avg} + 0.05 \varepsilon_{d,t}^h) \quad \forall t \in T \quad (2.30)$$

$$\Theta_{d,t}^{amb} = \Theta_{d,t}^{avg} + \varepsilon_{d,t}^t \quad \forall t \in T \quad (2.31)$$

To differentiate the PV system among the various households, $\tilde{C}_{d,t}$ is generated considering the average PV performance and some random noise (2.29). The performance of PV system $\rho_{d,t}^c$ follows a uniform distribution $U(0.8, 1.2)$, and the random noise $\varepsilon_{d,t}^c$ follows a normal distribution $\mathcal{N}(0, 1)$. The parameter $C_{d,t}^{avg}$ indicates the average state and is specific to the use-case. Moreover, it considers the difference in the households' loads as well, so $\tilde{U}_{d,t}$ is created considering the household's daily activities and random noise, which is formed as equation (2.30). The coefficient $\rho_{d,t}^h$ differentiates households' activities which follows a uniform distribution $U(0.7, 1.3)$ and the random noise $\varepsilon_{d,t}^h$ follows a normal distribution $\mathcal{N}(0, 1)$. The parameter $U_{d,t}^{avg}$ indicates the average value from the use-case. Finally, $\Theta_{d,t}^{amb}$ considers the environment random noise $\varepsilon_{d,t}^t$, which follows uniform distribution $U(-1.5, 1.5)$ to simply vary the outside temperature for the HVAC in different locations; $\Theta_{d,t}^{avg}$ indicates the initial data source from the use-case (2.31).

The optimization model presented is a mixed integer linear program, that can be difficult to solve for large number of households as it involves several discrete decisions and time steps. However, the problem is decomposable to local communities once constraint (2.3) is adjusted to the local community level and thus the scale of the computational challenge can be reduced dramatically. For instance, the problem decomposes to the number of local communities (i.e., number of energy storage) and each local community's operation can be optimized independently. Therefore, the optimal cost for the aggregator would be equal to the summation of the optimal cost for each local community independently, which means the objective function of the cost optimization could be changed to (2.32) and the

problem becomes decomposable over the number of local communities that are allocated to one CES each.

$$\min \sum_{t \in T} \Pi_t \Delta_T A_t = \min \sum_{e \in E} \sum_{r \in R_e} \sum_{t \in T} \Pi_t \Delta_T H_{r,t} \quad (2.32)$$

This significantly reduces the complexity of the problem and allow the solution of the operations of multiple communities in parallel. This is particularly possible in the case of CES-diverse as the local communities (i.e., households connected to the same energy storage) will have very similar power consumption profiles and thus A^{\max} can be divided by the number of local communities and replaced in constraint (2.3).

In summary, the general optimization problem can be displayed as follows:

$$\begin{aligned}
[\text{ESS-OPT}] \quad & \min \sum_{t \in T} \Pi_t \Delta_T A_t \\
\text{s.t.} \quad & A^{\min} \leq A_t \leq A^{\max} && (\text{Aggregator}) \\
& A_t = \sum_{r \in R} H_{r,t} && (\text{Aggregator}) \\
& H_r^{\min} \leq H_{r,t} \leq H_r^{\max} && (\text{Households}) \\
& H_{r,t} = D_{r,t} - \sum_{d \in D_r} \tilde{C}_{d,t} + \sum_{e \in E_r} (S_{r,e,t}^{ch} - S_{r,e,t}^{dis}) && (\text{Households}) \\
& D_{r,t} = \sum_{d \in D_r} \tilde{U}_{d,t} + \sum_{d \in D_r} \sum_{k=0}^{L-1} i_{d,t-k} \tilde{I}_{d,k} + \sum_{d \in D_r} (\theta_{d,t}^c + \theta_{d,t}^h) && (\text{Devices}) \\
& \sum_{t=0}^{|T|-1} i_{d,t} = 1 && (\text{Devices}) \\
& \Theta_{d,t+1} = a_d \Theta_{d,t} + (1 - a_d) (\Theta_{d,t}^{amb} - \Theta_{d,t}^m) && (\text{Devices}) \\
& \Theta_{d,t}^m = R_d \eta_d (\theta_{d,t}^c - \theta_{d,t}^h) && (\text{Devices}) \\
& t_{d,t}^c \theta_d^{\min} \leq \theta_{d,t}^c \leq t_{d,t}^c \theta_d^{\max} && (\text{Devices}) \\
& t_{d,t}^h \theta_d^{\min} \leq \theta_{d,t}^h \leq t_{d,t}^h \theta_d^{\max} && (\text{Devices}) \\
& t_{d,t}^c + t_{d,t}^h \leq 1 && (\text{Devices}) \\
& \Theta_d^{set} - \gamma \leq \Theta_{d,t} \leq \Theta_d^{set} + \gamma && (\text{Devices}) \\
& \Theta_{d,T} = \Theta_d^{set} && (\text{Devices}) \\
& B_e^{\min} \leq B_{e,t} \leq B_e^{\max} && (\text{Energy Storage}) \\
& S_{e,t}^{ch} = \sum_{r \in R_e} S_{r,e,t}^{ch} && (\text{Energy Storage}) \\
& S_{e,t}^{dis} = \sum_{r \in R_e} S_{r,e,t}^{dis} && (\text{Energy Storage}) \\
& \Delta_T (\eta^{ch} S_{e,t}^{ch} - \frac{1}{\eta^{dis}} S_{e,t}^{dis}) = B_{e,t} - B_{e,t-1} && (\text{Energy Storage}) \\
& S_e^{ch.min} \leq S_{e,t}^{ch} \leq S_e^{ch.max} && (\text{Energy Storage}) \\
& S_e^{dis.min} \leq S_{e,t}^{dis} \leq S_e^{dis.max} && (\text{Energy Storage}) \\
& s_{r,e,t}^{ch} S_e^{ch.min} \leq S_{r,e,t}^{ch} \leq s_{r,e,t}^{ch} S_e^{ch.max} && (\text{Energy Storage}) \\
& s_{r,e,t}^{dis} S_e^{dis.min} \leq S_{r,e,t}^{dis} \leq s_{r,e,t}^{dis} S_e^{dis.max} && (\text{Energy Storage}) \\
& s_{r,e,t}^{ch} + s_{r,e,t}^{dis} \leq 1 && (\text{Energy Storage}) \\
& s_{r,e,t}^{ch}, s_{r,e,t}^{dis}, i_{d,t}, t_{d,t}^c, t_{d,t}^h \in \{0, 1\}
\end{aligned}$$

2.4 Software and User Interface

In order to apply the proposed methodology to realistic use cases, a software with a user interface is developed where the user can adjust the parameters and visualize the computational results, see Figure 2.4:

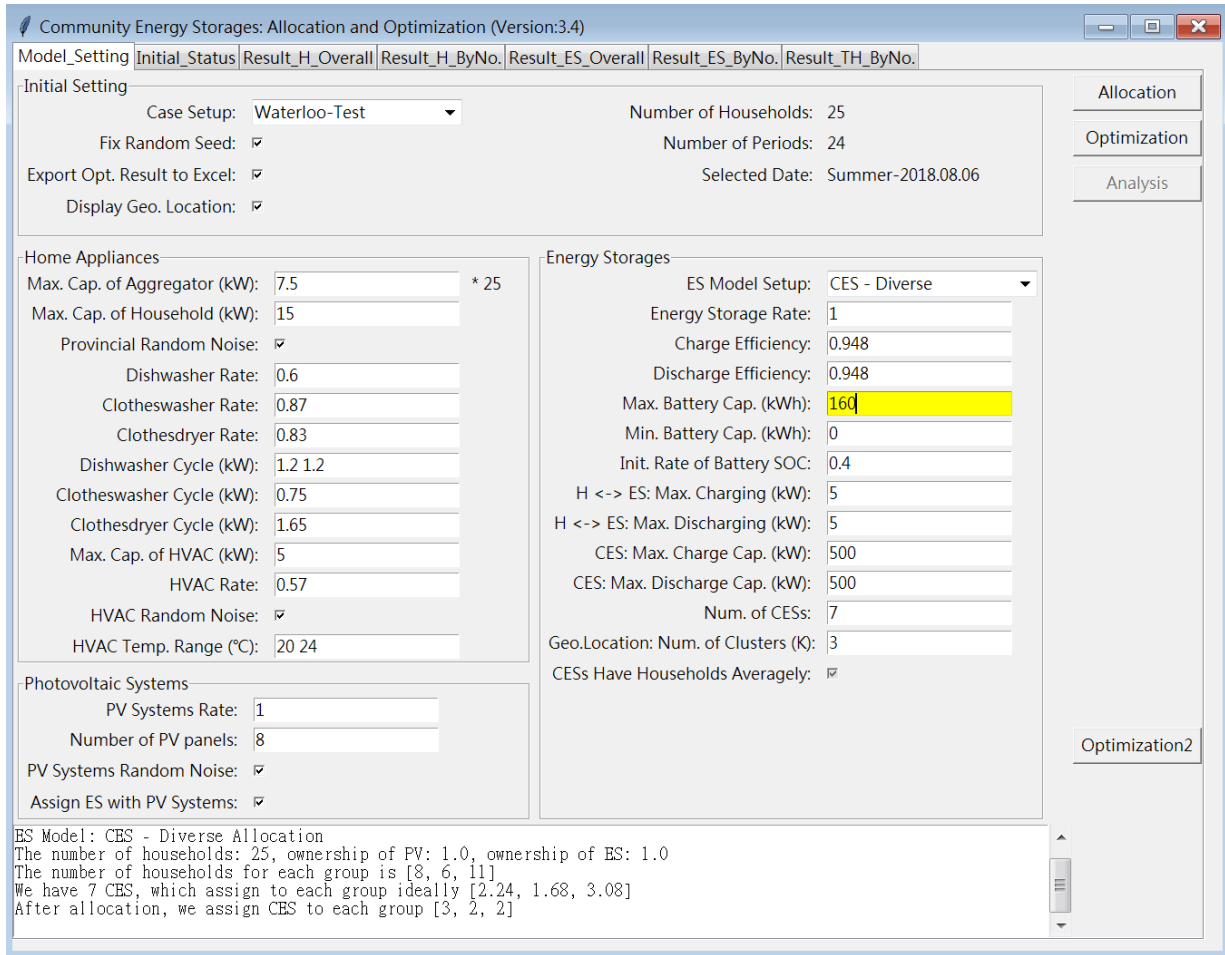


Figure 2.4: User interface.

The interface has multiple forms for the user. The user interface is designed to control the model, where the user can enter all the parameters and execute the process step by step. There are three options for execution: the first one “Allocation” executes the action

of allocating households to a community, and also assigns home appliances, PV systems, energy storages to households based on the parameter settings. After completing the allocation step, the second option “Optimization” runs the optimization model to obtain the minimal operational cost using ILOG CPLEX Optimization Studio 12.8. Finally, based on the computational results, the third one “Analysis” can be used to review key performance indexes, schedules of appliances for each household, and energy storage as seen in Figure 2.4.

The first form “Initial Setting” controls the basic setting of the use-case, which includes time period Δ_T and T , provincial load $U_{d,t}^{avg}$, curtailable load $C_{d,t}^{avg}$, energy price Π_t , and ambient temperature $\Theta_{d,t}^{avg}$, see Figure 2.4. Also, the households’ coordinates and number of household is controlled in that form. The user can control the random seeds of the random noise and the device’s performance easily, such as $\rho_{d,t}^c$, $\varepsilon_{d,t}^c$, etc., and control the random seeds of the random allocation option as well. The output of the CPLEX optimization model can be saved if this option is selected. In addition, the allocation results on a given geographical location can be displayed if the function is selected using the Open Street Map.

Then, the form “Home Appliances” in Figure 2.4 focuses on calculating $D_{r,t}$. Using this form, one can adjust all the parameters of home appliances, including the limitation of specification (e.g., A^{\min} , A^{\max} , etc.), cycle time and power consumption of uninterruptible load, indoor temperature setting, ownership rate of home appliances, etc. Based on the input, the number of variables for each type of appliances and the upper and lower bound of variables can be determined.

Additionally, the form “Photovoltaic Systems” in Figure 2.4 controls the parameters of the PV system. It includes the ownership rate of the PV system, and the number of the solar PV panels installed in each household. The household owner has a higher motivation to install or be connected to an energy storage when it has a PV system, and vice versa. When this option is selected, the allocation of energy storage would have higher priority to be assigned to the household which has a PV system, and vice versa.

Moreover, the form “Energy Storage” in Figure 2.4 focuses on the allocation options and parameters of energy storage. The allocation options can be selected in this form, including PES-single, CES-random, CES-homogeneous, CES-diverse. Also, the ownership rate, round-trip efficiency, battery capacity, initial status of the battery before optimization, rated continuous power capacity can be controlled in this form. The parameter K for the k -mean method can be determined as well, and there are some fool-proof mechanisms on the input of ownership rate, number of CES, and K to avoid incorrect input. For example, the number of CES can not be smaller than K . Finally, the assumption which all the CESs

in one community are assigned to almost the same number of households, can be controlled in this form. If the function does not be selected, the allocation would not consider the number of households and assign the households to CESs based on the random seed.

The status after community setting and allocation can be reviewed in Figure 2.5 and 2.6. In Figure 2.5, it can review basic input from the parameters, i.e., energy price Π_t , and ambient temperature Θ_t^{avg} , average provincial load of households C_t^{avg} , and average PV power generation from PV systems U_t^{avg} . Figure 2.6 can review the allocation status for all the households, including the number of home appliances, PV system, and energy storage.

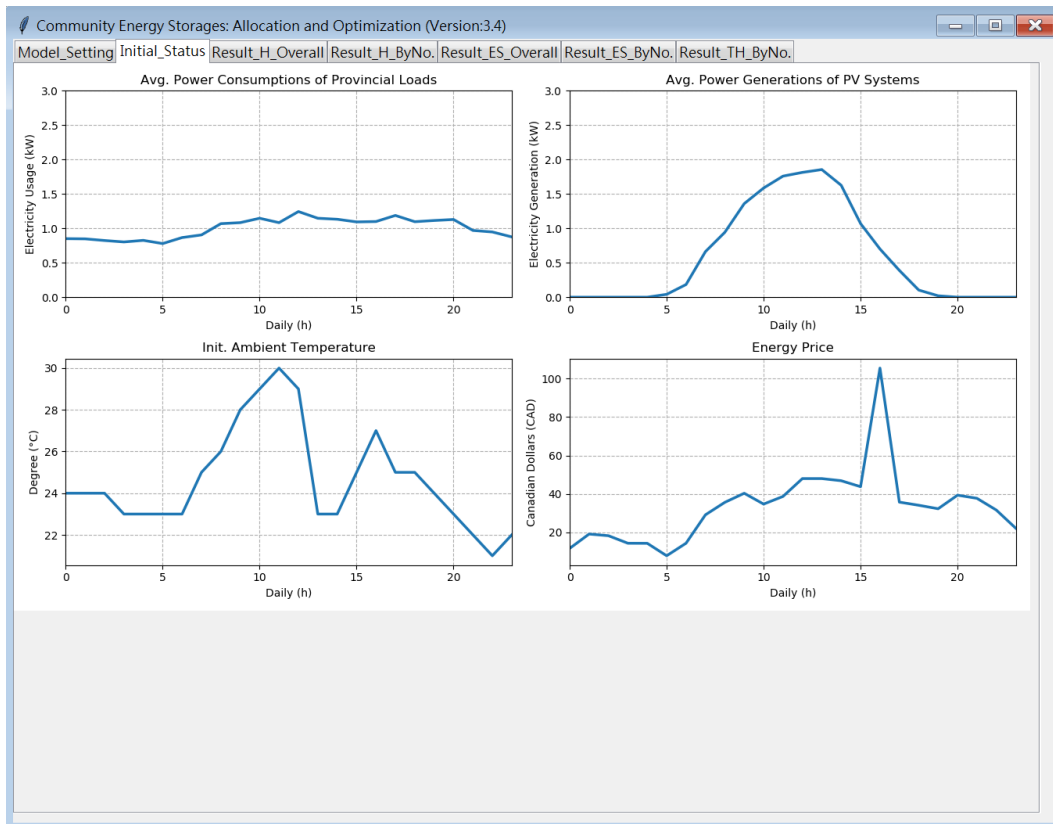


Figure 2.5: User interface: initial status.

Model_Setting	Initial_Status	Result_H_Overall	Result_H_ByNo.	Result_ES_Overall	Result_ES_ByNo.	Result_TH_ByNo.	EnergyStorage
Household	Provincial	DishWasher	ClothesWasher	ClothesDryer	HVAC	PVSystem	
0	0	nan	42	77	83	100	123
1	1	33	52	64	nan	107	124
2	2	39	44	nan	nan	98	122
3	3	27	51	80	nan	108	122
4	4	nan	57	74	95	99	123
5	5	28	50	63	86	114	123
6	6	26	43	66	85	110	122
7	7	37	45	82	84	102	124
8	8	29	56	78	nan	109	128
9	9	nan	47	69	93	117	127
10	10	32	41	71	nan	115	128
11	11	36	49	81	96	104	128
12	12	nan	nan	79	nan	103	127
13	13	38	54	73	nan	119	128
14	14	nan	nan	nan	92	101	128
15	15	nan	59	nan	87	113	127
16	16	30	61	nan	nan	105	127
17	17	nan	55	72	90	118	127
18	18	25	58	70	89	120	127
19	19	35	48	76	nan	97	125
20	20	nan	53	68	94	116	126
21	21	nan	60	67	91	106	126
22	22	31	nan	75	nan	111	126
23	23	nan	40	62	nan	112	125
24	24	34	46	65	88	121	125

Figure 2.6: User interface: allocation.

The computational results can be analyzed graphically. In one form, the computational results of selected variables for each household can be checked to confirm the optimal schedule in a given period, e.g., the household power consumption $H_{r,t}$ at each period t , the charging power to the energy storage $S_{r,e,t}^{ch}$, etc., see Figure 2.7. Also, the schedule of the HVAC for the household can be reviewed graphically, see Figure 2.8.

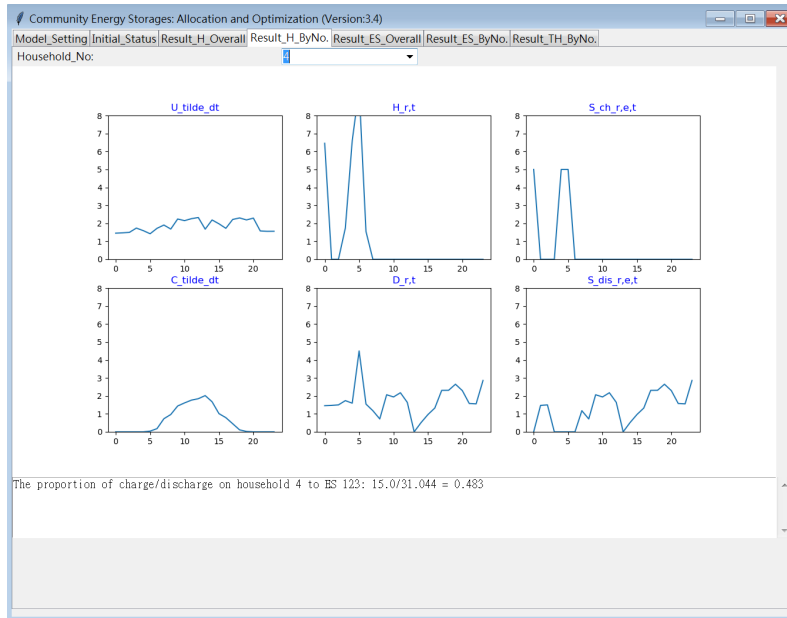


Figure 2.7: User interface: the optimal schedule of the household.

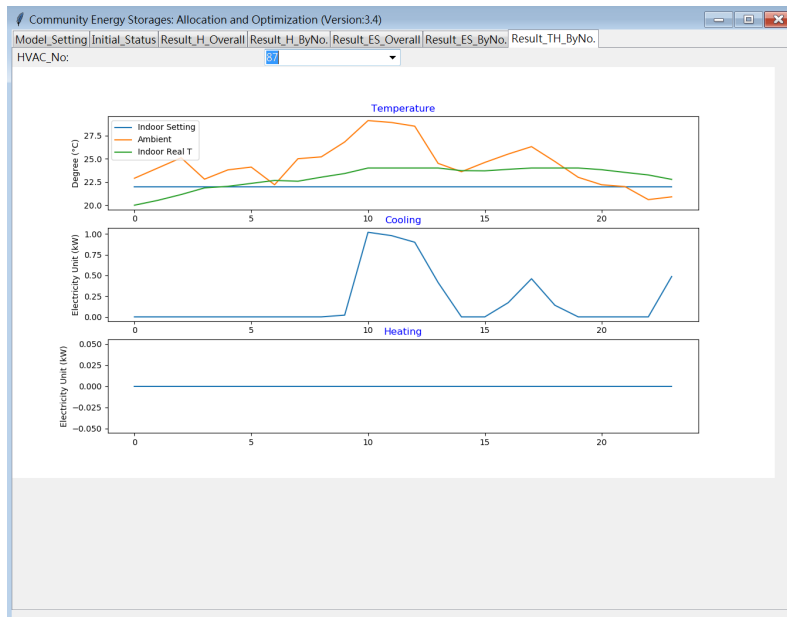


Figure 2.8: User interface: performance of the HVAC for the household.

Finally, the charging and discharging schedule of each energy storage can be reviewed, and the battery state of charge in each period can be checked as well, see Figure 2.9. For each energy storage, the detailed charging and discharging power from the households at each period can be checked graphically. Based on the charging and discharging proportion from each household, the minimal and maximal ratio are shown as well, see Figure 2.10.

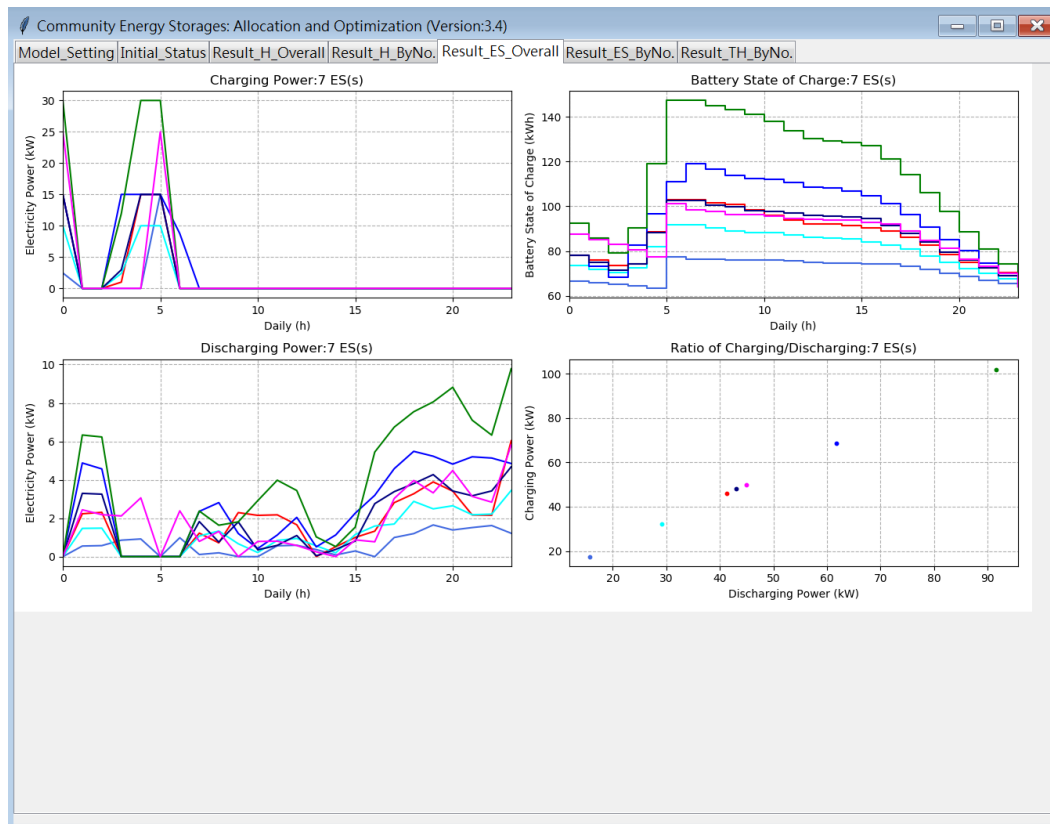


Figure 2.9: User interface: overall review of energy storages.

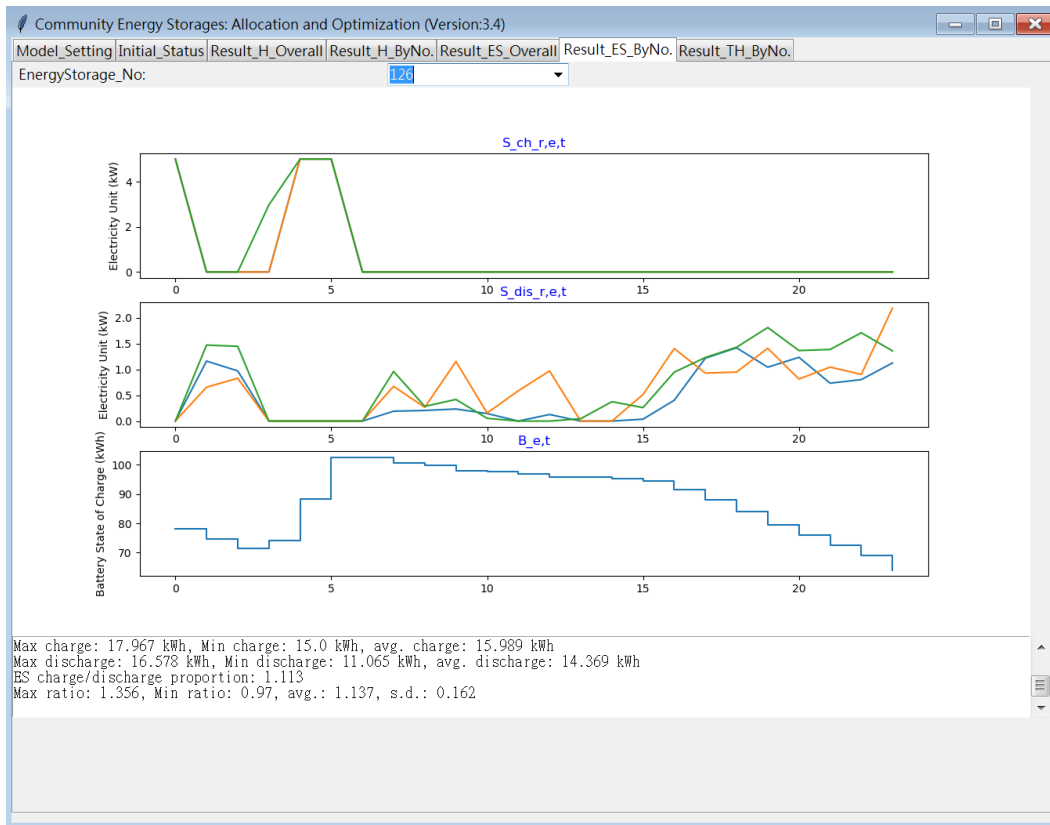


Figure 2.10: User interface: detailed schedule of single energy storage.

Chapter 3

Case Study

Two different use cases are selected to test the results of the proposed methods; one is Ennis, Ireland, the other one is Waterloo, Canada. Next, a detailed description of the data of the two use cases is given followed by the computational results and analysis.

3.1 Case 1: Ennis, Ireland

The first use case is a region in Ennis, Ireland. It is a typical community in Ireland and it contains 1024 households.

3.1.1 Parameter Setting

The ownership rates of home appliances for the households in Ennis are displayed in Table 3.1. All households are assumed to use necessary home appliances (e.g., refrigerator, lighting) which are categorized as provincial load. Also, the ownership rates of dish washer, clothes washer, clothes dryer are taken from SEAI, Energy in Residential Sector 2018 Report [36]. Since the demand of air conditioner is significantly low in Ireland [37], the ownership rate of air conditioner is assumed low in summer time; the ownership rate of space heating using electricity is also calculated from SEAI, Energy in Residential Sector 2018 Report [36]. Moreover, a rooftop solar panel is assumed to be the main PV system for a household, and households would use either PES or CES based on allocation options. The ownership rates of PV systems and energy storages are varied to simulate different scenarios.

Table 3.1: Ownership rates of home appliances in Ennis, Ireland

Devices	Category	Ownership rate
Dish washer	Uninterruptible load	65%
Clothes washer	Uninterruptible load	98%
Clothes dryer	Uninterruptible load	65%
Air conditioner	Thermal load	1%
Hydro space heating	Thermal load	7%
Rooftop solar	PV system	0% - 100%
PES or CES	Energy storage	0% - 100%
Others	Provincial load	100%

To represent a real scenario, parameters are created using the record in July 8, 2018 to represent a summer day and November 30, 2018, which is a typical winter day without snowing. The parameters are displayed in Table 3.2.

Table 3.2: Parameters of home appliances in Ennis, Ireland

Category	Parameters	Data Source, Assumptions
Period time	$\Delta_T = 1, T = 24$	Simulating one day
Energy price	Π_t	N2EX Day Ahead Auction Prices
Aggregator	$A^{\min} = 0, A^{\max} = 7.5 \times 1024$	
Household	$H_r^{\min} = 0, H_r^{\max} = 15$	
Provincial load	$U_{d,t}^{avg}$	CER, Electricity Smart Metering Technology Trials Findings Report
Dish washer	$\tilde{I}_{d,t} = [0.83, 0.83, 0.83, 0.83]$	Eco50° program, Whirlpool, WFO-3P33-DL-X
Clothes washer	$\tilde{I}_{d,t} = [0.78, 0.78, 0.78, 0.13]$	Standard 60°C cotton program, Half load, Whirlpool, FWG91284W
Clothes dryer	$\tilde{I}_{d,t} = [1.16, 1]$	Partial load, Whirlpool, HSCX-90423
Indoor temp. setting	$\Theta_t^{set} = [18, 21]$	Recommended temp. in the living room
Ambient temp.	$\Theta_{d,t}^{avg}$	ie.freemeteo.com
AC or Heating	$\theta_d^{\min} = 0, \theta_d^{\max} = 3.5, \gamma = 2$ $C_d = 2.5, R_d = 2, \eta_d = 2.5$	
PV system	$C_{d,t}^{avg}$	Courtown, Corporate Wexford, Ireland, Suntech Hypro STP285S-20/Web modules, 8 pcs
PES battery	$B_e^{\max} = 13.5, B_e^{\min} = 0$	Tesla Powerwall
PES efficiency	$\eta^{ch} = 0.948, \eta^{dis} = 0.948$	Tesla Powerwall
PES charging	$S_e^{ch, \max} = 5, S_e^{ch, \min} = 0$	Tesla Powerwall
PES discharging	$S_e^{dis, \max} = 5, S_e^{dis, \min} = 0$	Tesla Powerwall
CES battery	$B_e^{\max} = 250, B_e^{\min} = 0$	eCamion Community Energy Storage
CES efficiency	$\eta^{ch} = 0.948, \eta^{dis} = 0.948$	eCamion Community Energy Storage
CES charging	$S_e^{ch, \max} = 500, S_e^{ch, \min} = 0$	eCamion Community Energy Storage
CES discharging	$S_e^{dis, \max} = 500, S_e^{dis, \min} = 0$	eCamion Community Energy Storage
CES charging	$S_{r,e}^{ch, \max} = 5, S_{r,e}^{ch, \min} = 0$	eCamion Community Energy Storage
CES discharging	$S_{r,e}^{dis, \max} = 5, S_{r,e}^{dis, \min} = 0$	eCamion Community Energy Storage
Initial battery SOC	$B_{e,-1} = 40\%$	
Final battery SOC	$B_{e,23} = 40\%$	

The simulation period is one day, which sets $\Delta_T = 1, |T| = 24$. The electricity price at a period t , Π_t , is extracted from N2EX Day Ahead Auction Prices [38], see Figure 3.1. For the aggregator, the capacity of power consumption is assumed $A^{\min} = 0$ kW, $A^{\max} = 7.5kW \times 1024$, and $H_r^{\min} = 0$ kW and $H_r^{\max} = 15$ kW for each household.

The provincial load $U_{d,t}^{avg}$ is taken from CER, Electricity Smart Metering Technology Trials Findings Report [39], which contains data of regular households without smart meters, see Figure 3.1.

The home appliances are categorized as uninterruptible loads with A++ or better on

the certification of energy labeling in the EU. A dish washer would operate 4 hours with 0.833 kW in each hour using the Eco50° program from Whirlpool, WFO-3P33-DL-X model. A washer operates on 0.78 kW in the first three hours and 0.13 kW in the last hour on the standard 60°C control program at half load from Whirlpool, FWG91284W model. A dryer usually operates 112 minutes with 1.16 kWh at partial load from Whirlpool, HSCX-90423 model, which assumes that it consumes 1.16 kW in the beginning hour and 1 kW in the last hour. Based on the information above, L and $\tilde{I}_{d,t}$ are determined accordingly.

Moreover, considering the recommended temperature for the living room from Ireland government, the thermal load assumes the indoor temperature setting of air conditioner or hydro space heating Θ_t^{set} in the range [18, 21] °C. The ambient temperature record $\Theta_{d,t}^{avg}$ is taken from ie.freemeteo.com, see Figure 3.1. For each thermal load, the capacity of power consumption is assumed to be between $\theta_d^{\min} = 0$ kW and $\theta_d^{\max} = 3.5$ kW considering normal usage. Based on the thermodynamic model, the following parameters are given: thermal capacitance $C_d = 2.5$ kWh/°C, thermal resistance $R_d = 2$ °C/kW, and the working efficiency factor $\eta_d = 2.5$ [9]. The tolerance between indoor and ambient temperature is assumed $\gamma = 2$ °C.

The PV system consists of rooftop solar panel, which considers the specification of Suntech Hypro STP285S-20/Web modules, and assumes that each household installs 8 panels if it owns a PV system. $C_{d,t}^{avg}$ is taken from the solar PV system project of Courtown, Corporate Wexford in Ireland [40], see Figure 3.1.

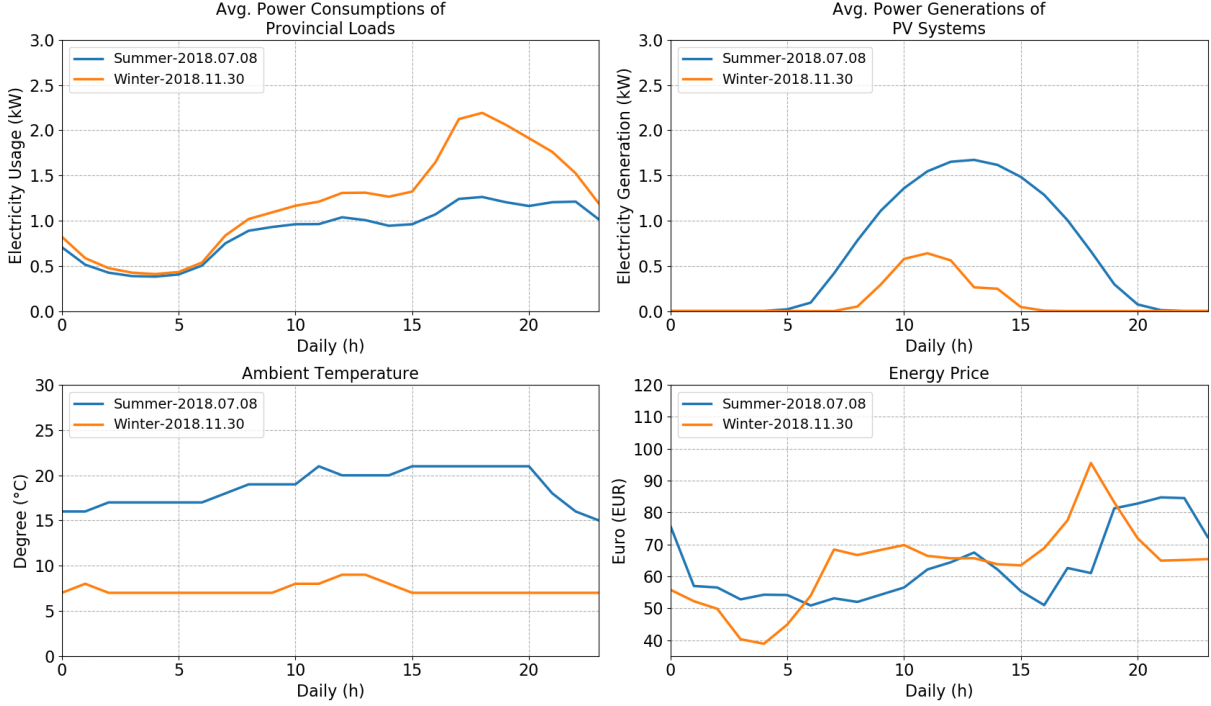


Figure 3.1: Daily charts for the parameters in Ennis.

The parameters of PES are that of the specification of Tesla Powerwall [41]. The battery state of charge is $B_e^{\max} = 13.5$ kWh and $B_e^{\min} = 0$ kWh. Efficiencies of charging and discharging are $\eta^{ch} = 0.948$ and $\eta^{dis} = 0.948$ respectively, yielding a 90% round-trip efficiency. The power capacity of PES is $S_e^{ch.\max} = S_e^{dis.\max} = 5$ kW and $S_e^{ch.\min} = S_e^{dis.\min} = 0$ kW.

Similarly, the parameters of CES are according to the specification of eCamion Community Energy Storage [42]. The battery capacity B_e^{\max} that can be achieved is 250 kWh and $B_e^{\min} = 0$ kWh; the power capacity from households is $S_{r,e}^{ch.\max} = S_{r,e}^{dis.\max} = 5$ kW and $S_{r,e}^{ch.\min} = S_{r,e}^{dis.\min} = 0$ kW. The rated continuous power capacity of CES is $S_e^{ch.\max} = S_e^{dis.\max} = 500$ kW and $S_e^{ch.\min} = S_e^{dis.\min} = 0$ kW, and efficiencies of charging and discharging are formed $\eta^{ch} = 0.948$ and $\eta^{dis} = 0.948$, yielding a 90% round-trip efficiency as well.

Finally, the initial battery status $B_{e,-1}$ and the end battery status $B_{e,23}$ are assumed to be 40% of maximum battery state of charge. B_e^{\max} for CES would be an important factor for the analysis, which means the maximum battery capacity will vary when the proposed

approach analyzes the suitable battery size.

3.1.2 Community Setting

The first step before running the algorithm is to form communities which are built by using k -mean approach. The geographical locations are used to cluster the households using their longitude and latitude locations. In this case, $K = 3$ is used to form three communities which refers to the distance limitation of CES and the road intersection, and the size of these communities are 469, 297, 258, respectively, see Figure 3.2.

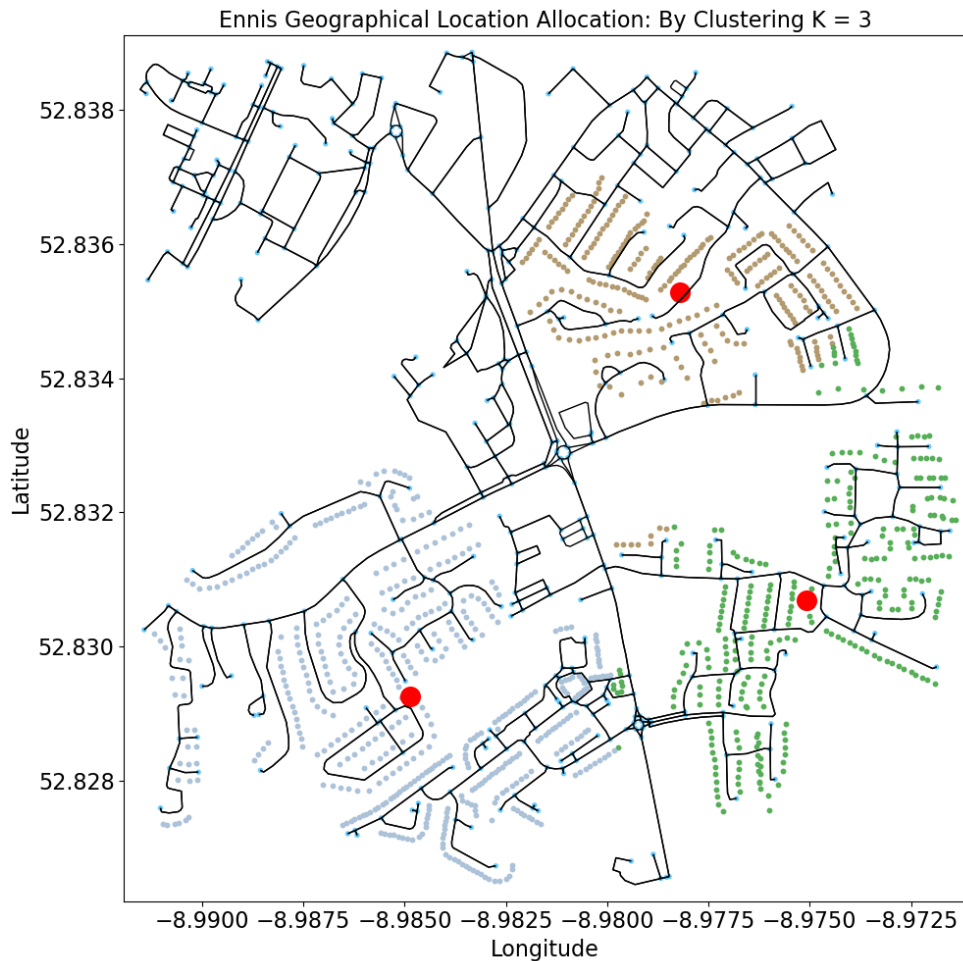


Figure 3.2: Region map and households' locations in Ennis, Ireland.

3.1.3 Computational Results

3.1.3.1 Features for PES

When households install PV systems and PESs, their electricity operational cost can decrease significantly. Figure 3.3 indicates the percentage of operational cost reduction for the aggregator when the ownership rate of PV system and PES increase. From Figure 3.3, the operational cost decreases linearly if the ownership rates increase. In the summer period, if all the households own the PV system and PES, the maximum cost reduction can reach to 55.45%. The PV systems can generate a substantial amount of power to the households in summer, and therefore the cost reduction would be more significant when the ownership rate of the PV system increase. In the summer day, the cost reduces to 10.34% when all the households own the PES without installing the PV system, but the cost reduces more to 45.91% when all the households own the PV systems without installing the PES. In contrast, the power generation of the PV systems in the winter day cannot provide enough support to the households, and the cost reduction is only 6.95% when all the households own the PV systems without installing the PES. However, the reduction remains at a similar level compared to the summer day when all the households own the PES without installing the PV system (around 12.68%). Thus, PESs can provide a stable cost reduction for the households, and PV systems can help households reduce their costs in the summer. Households can have substantial cost reduction when both devices are installed.

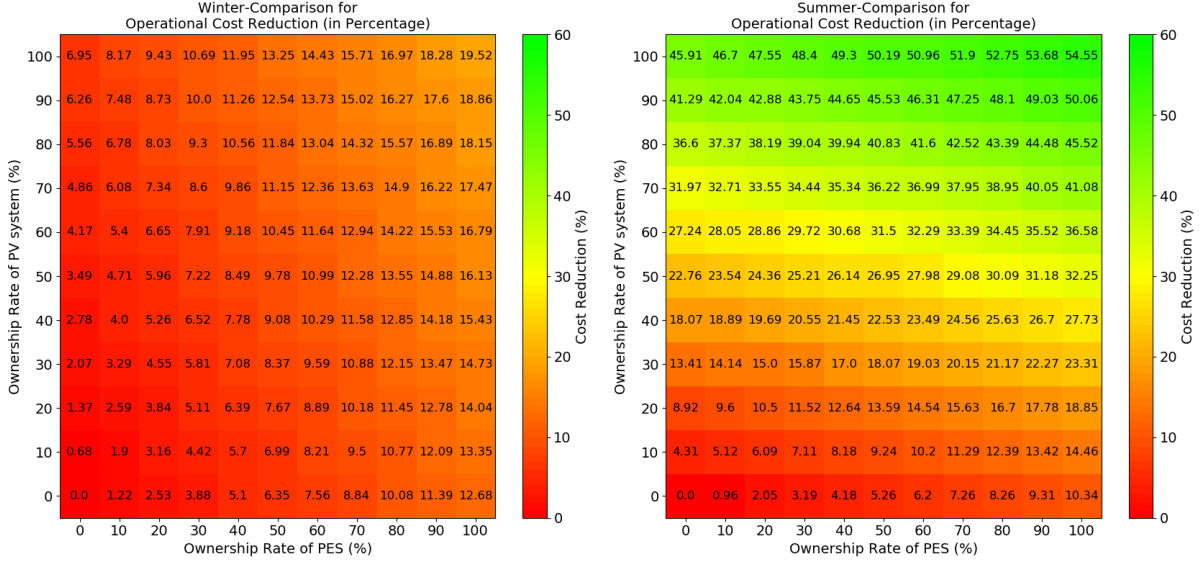


Figure 3.3: Operational cost reduction varying the ownership rate of PV system and PES in Ennis.

Additionally, the ratio of storing power and consuming power from the energy storage is defined as (3.1).

$$\Omega = \sum_{t=0}^{|T|-1} S_{e,t}^{ch} / \sum_{t=0}^{|T|-1} S_{e,t}^{dis} \quad (3.1)$$

In this case, the ratio Ω is the same for all the households whether in summer or winter, which is 1.113. It implies that when the households know exactly the energy price and their power consumption and generation are predictable, the ratio is determined only by the efficiencies of charging and discharging; given the deterministic information, they can calculate the optimal charging/discharging ratio and decide when they should charge and discharge their own PES. When the efficiencies change, this ratio will change; the value of Ω does not depend on the specification of the PV system, the ownership of home appliances, and the ownership of PV system, etc.

From the scheduling point of view, all the PESs have similar activities on charging, discharging, and similar battery state of charge in specific periods, which means the behavior patterns of the households would be almost the same to avoid spending money when the energy price is high. Figure 3.4 shows the features of charging and discharging in the

selected days which the households have the PV system and the PES. It indicates that the households would charge the PES when the energy price is low and discharge when the price is high assumed the maximum battery capacity is affordable; the points in the scatter chart are located on the line $y = x/1.113$, meaning that the ratio is the same.

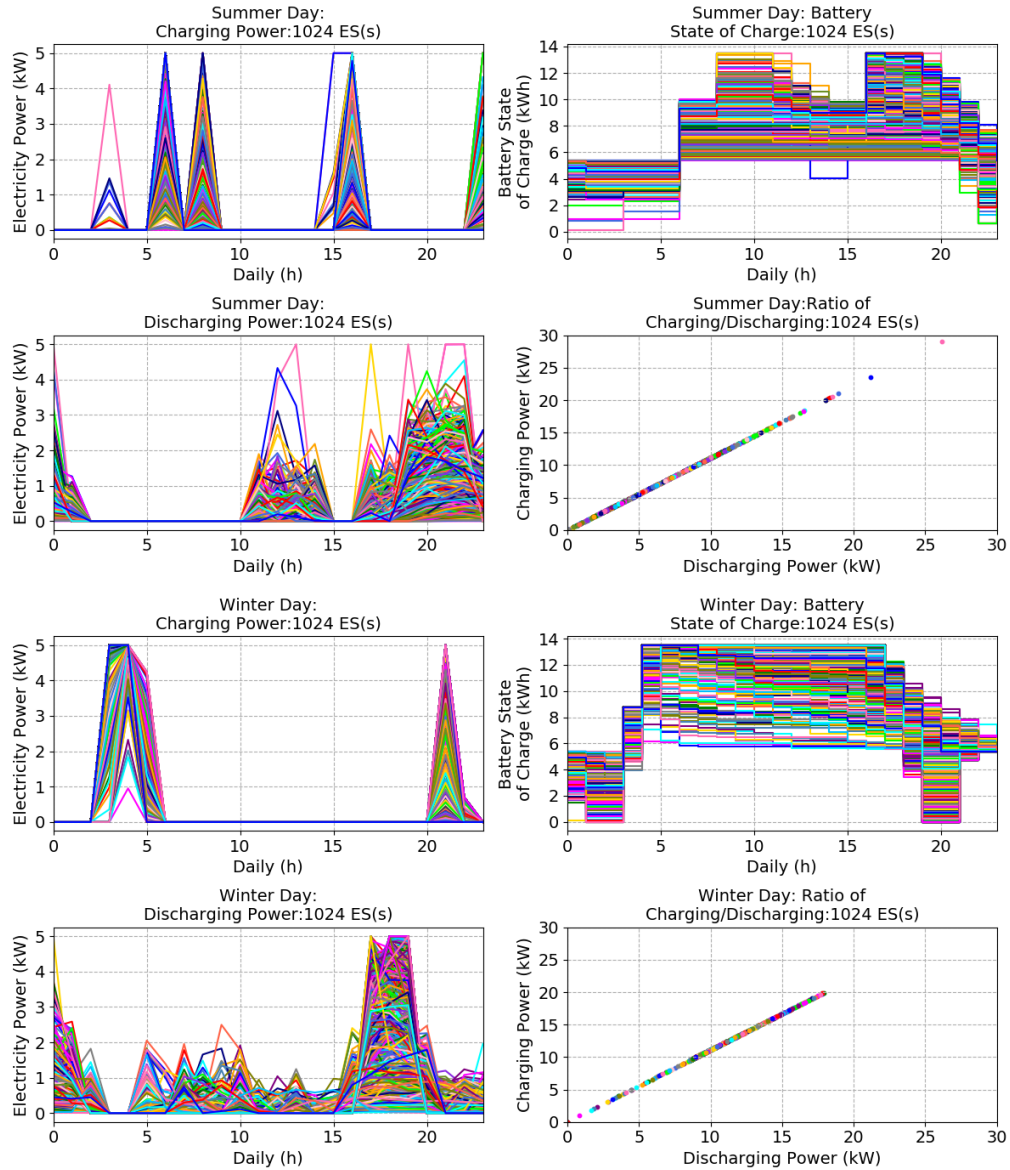


Figure 3.4: Features for charging and discharging of PES.

Finally, when the households choose PES-single option, they would optimize their own power consumption and generation without considering their neighbors in the community, meaning that surplus power generation from each household cannot be used by its neighbors, and thus the household cannot share or receive any resources for its community. In contrast, when households select to install CESs, the surplus power can share to their communities, meaning that households can have more flexibility from CES to reduce the operational cost. However, optimal number of CES and battery capacity should be determined by the size of community to avoid wasting resources.

3.1.3.2 Determining Battery Capacity of CES

From the specification, the maximum battery capacity of CES e is $B_e^{\max} = 250$ kWh. However, to achieve the best economic benefit for the community, the number and the capacity of CESs should be examined. Therefore, the battery capacity and the number of CESs are varied in this section to simulate all possible scenarios and to obtain optimal battery capacity. Assuming the ownership rate of CESs and PV system is 100%, the average battery capacity for each household is simply calculated as (3.2).

$$\text{Avg. Battery Capacity Per Household} = \frac{|E| \cdot (B^{\max})}{|R|} \quad (3.2)$$

Different battery capacities and number of CESs are considered and the average battery capacity per household is given in Table 3.3. The value of B^{\max} has six options with a minimum value of 40 kWh and a maximum value of 240 kWh and the number of CESs varies from 10 to 150.

Table 3.3: Average battery capacity for each household in Ennis

		CES maximum battery capacity (kWh)					
		40	80	120	160	200	240
Number of CES	10	0.391	0.781	1.172	1.563	1.953	2.344
	20	0.781	1.563	2.344	3.125	3.906	4.688
	30	1.172	2.344	3.516	4.688	5.859	7.031
	40	1.563	3.125	4.688	6.250	7.813	9.375
	50	1.953	3.906	5.859	7.813	9.766	11.719
	60	2.344	4.688	7.031	9.375	11.719	14.063
	70	2.734	5.469	8.203	10.938	13.672	16.406
	80	3.125	6.250	9.375	12.500	15.625	18.750
	90	3.516	7.031	10.547	14.063	17.578	21.094
	100	3.906	7.813	11.719	15.625	19.531	23.438
	110	4.297	8.594	12.891	17.188	21.484	25.781
	120	4.688	9.375	14.063	18.750	23.438	28.125
	130	5.078	10.156	15.234	20.313	25.391	30.469
	140	5.469	10.938	16.406	21.875	27.344	32.813
	150	5.859	11.719	17.578	23.438	29.297	35.156

Next, for a given capacity and number of CESs, the optimization problem presented in Section 2.3 is solved where each household connects to one CES using the random allocation option and each household owns the PV system. The operational cost of the aggregator is an output of the model. Figure 3.5 indicates that when the number of CES and the size of battery capacity increase, the overall operational cost decreases. For example, in the summer day, when the size of battery capacity is 160 kWh and the number of CES is larger than 56 units, the operational cost would be lower than PES-single option. Similarly, the same observation occurs when the size of battery capacity is 200 kWh and the number of CES is larger than 64 units in the winter day. Thus, if the households decide to install CESs, the average battery capacity for each household should be bigger than 12.66 kWh in the winter day and larger than 8.9 kWh in the summer day to make the operational cost lower. In other words, the range of average battery capacity for each household should be within [12.66, 13.5] and [8.9, 13.5] to achieve better economic benefit in the winter and summer day, respectively. Thus, the PV systems can provide the CESs with more flexibility

to adjust the average battery capacity in the summer day in this case.

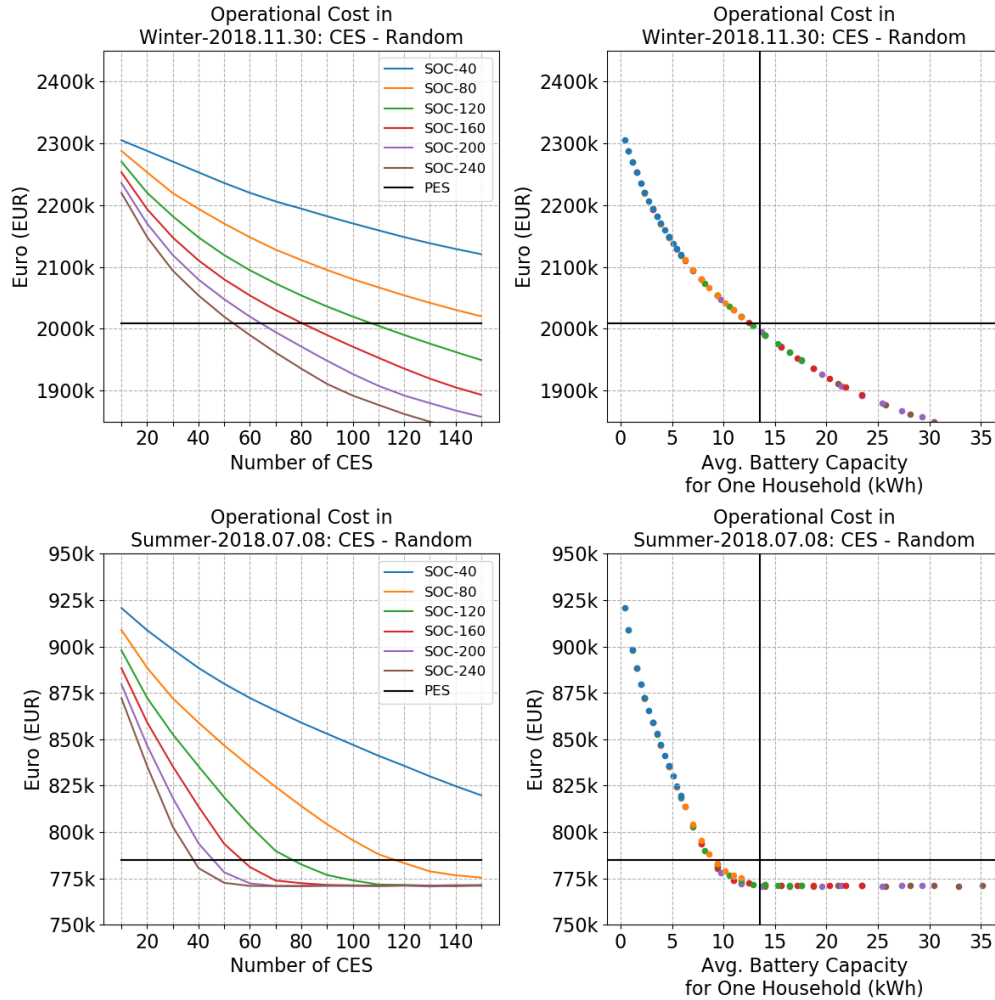


Figure 3.5: Operational cost varying battery capacity and number of CES.

Moreover, although operational costs can be reduced when the battery capacity of CES increases, the marginal utility is diminishing. In this case, the operational cost cannot decrease further when the average battery capacity of CES is bigger than 12.5 kWh in the summer day. It implies that households can select CESs with suitable average battery capacity instead of the biggest one to avoid wasted cost.

Finally, if considering capital cost, the households would have lower capital cost in-

stalling CES than installing PES individually. Based on the formula from [32], the capital cost of CES is calculated simply as (3.3):

$$\text{Capital Cost} = \text{Cell Cost} \cdot B^{\max} + \text{Init. Inverter Cost} \times \left(\frac{\text{C-rate} \cdot B^{\max}}{3} \right)^{0.7} \quad (3.3)$$

Based on the assumption [32], the capital cost is calculated based on battery properties that are given in Table 3.4. The capital cost of CES for each combination which achieves a similar or lower operational cost as that of the PES-single option is calculated and compared with the anticipated capital cost of PES (Tesla Powerwall quoted at \$6200 including the supporting hardware [32]). The capital cost of CES is much lower than PES as shown in Table 3.4.

Table 3.4: The capital costs of CES combinations

Property	Value of Function
Cell Cost	\$250/kWh
C-rate	0.5
Init. Inverter Cost	\$1500

Date	Number of CES	B^{\max}	Average Battery Cap.	Operational Cost	Capital Cost
Winter Day	120	108	12.656	2,007,758.49	4,601,330
Winter Day	160	81	12.656	2,007,624.53	4,724,038
Winter Day	200	65	12.695	2,006,981.23	4,840,211
Winter Day	240	54	12.656	2,007,574.82	4,915,993
Summer Day	80	116	9.063	784,008.62	3,274,105
Summer Day	120	76	8.906	784,240.49	3,344,477
Summer Day	160	57	8.906	783,752.18	3,440,427
Summer Day	200	46	8.984	782,622.28	3,548,377
Summer Day	240	38	8.906	784,055.09	3,590,524

Date	Number of PES	B^{\max}	Average Battery Cap.	Operational Cost	Capital Cost
Winter Day	1024	13.5	13.5	2,009,307.04	6,348,800
Summer Day	1024	13.5	13.5	784,987.53	6,348,800

In summary, the aggregator and thus households have a lower capital costs and operational costs when they install CES as opposed to having PES. There is also a trade off between the number of CES and the battery capacity, the capital cost is lower when having fewer CESs with a high battery capacity.

3.1.3.3 Allocation Options for CES

For different allocation options, a comparison of operational cost for each household is examined. Figure 3.6 states the comparison of operational cost among three allocation methods: CES-random, CES-diverse, and CES-homogeneous when the average battery capacity for each household increases. The result displays that the optimal costs of CES-diverse are slightly lower than the operational cost of CES-random, and the cost of CES-homogeneous is higher than the others. It implies that if the CES serves the households that have similar power consumption pattern, the performance is worse than if CES serves the households with different power consumption patterns.

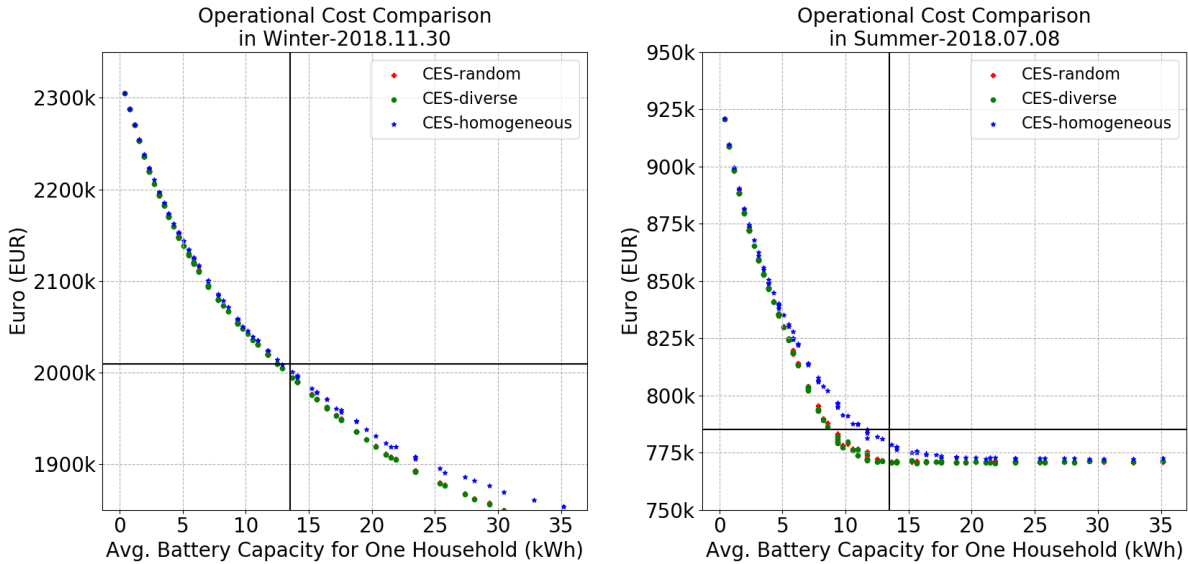


Figure 3.6: Operational cost for different CES allocation options.

Compared to the PES-single option, CESs have similar charging and discharging patterns but CES options are more stable whether in summer or winter. Figure 3.7 provides an example where 57 CESs each of size 160kWh are allocated and the operational cost

is similar to the PES-single option (Table 3.4). The charging, discharging, battery state of charge and the ratio of charging and discharging from different CESs are given on the summer day. The CES-diverse option causes the CESs to have almost the same patterns for charging, discharging and battery state of charge. In contrast, the CES-homogeneous option have different patterns on charging, discharging and battery state of charge. For the CES-random option, the patterns are between CES-diverse and CES-homogeneous.

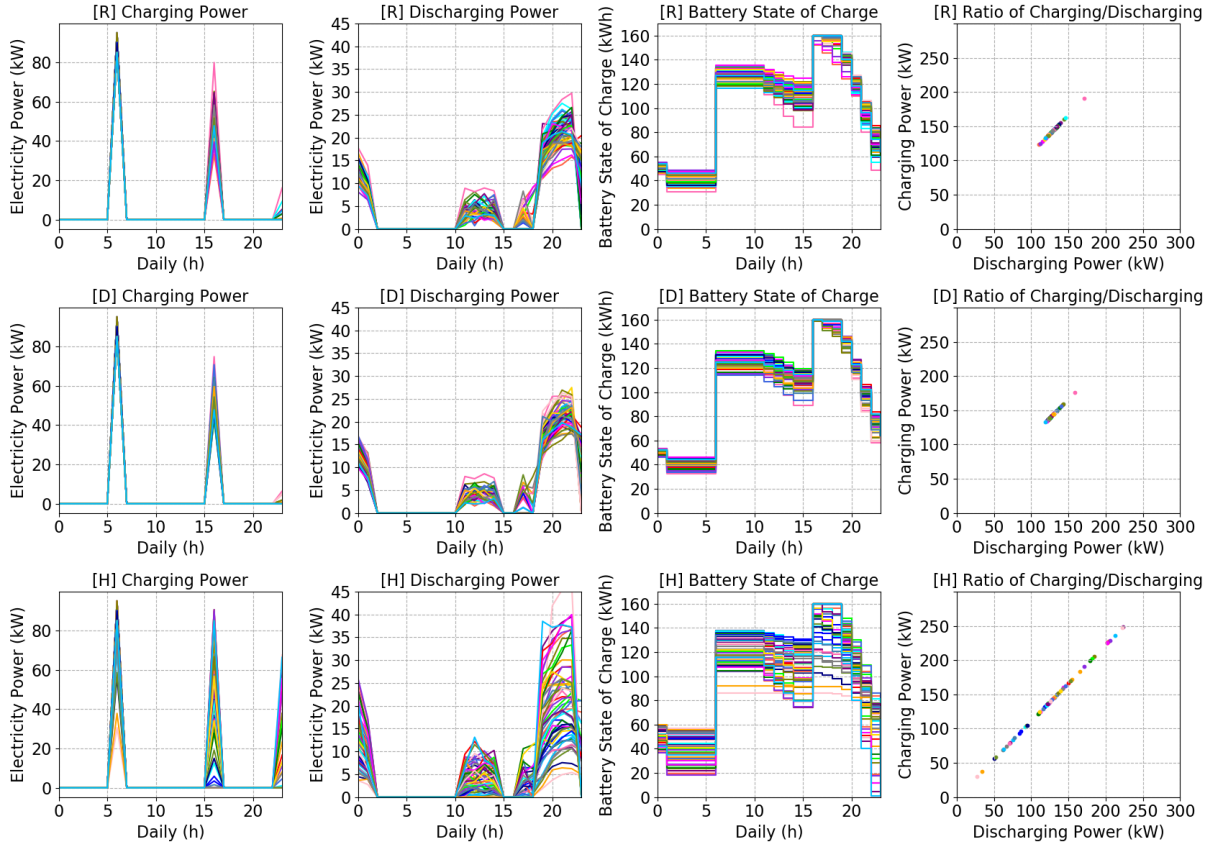


Figure 3.7: Comparing battery charging, discharging, state of charge, and ratio of charging vs discharging among different CES allocation options in summer: [R] CES-random [D] CES-diverse [H] CES-homogeneous.

Additionally, the sum of the loads at each period ($\sum_{r \in R_e} H_{r,t}$) of the households connected to each CES also show that the CES-diverse option causes the CESs to have almost

the same patterns in each period, and total household load ($\sum_{r \in R_e} H_r$) for each CES is similar to each other. In contrast, the operation pattern of the CES-homogeneous option and total household net load is significantly different for each CES, and the CES-random option is between CES-diverse and CES-homogeneous, see Figure 3.8. It implies that the CES-homogeneous option would cause some CESs to have heavier operation load.

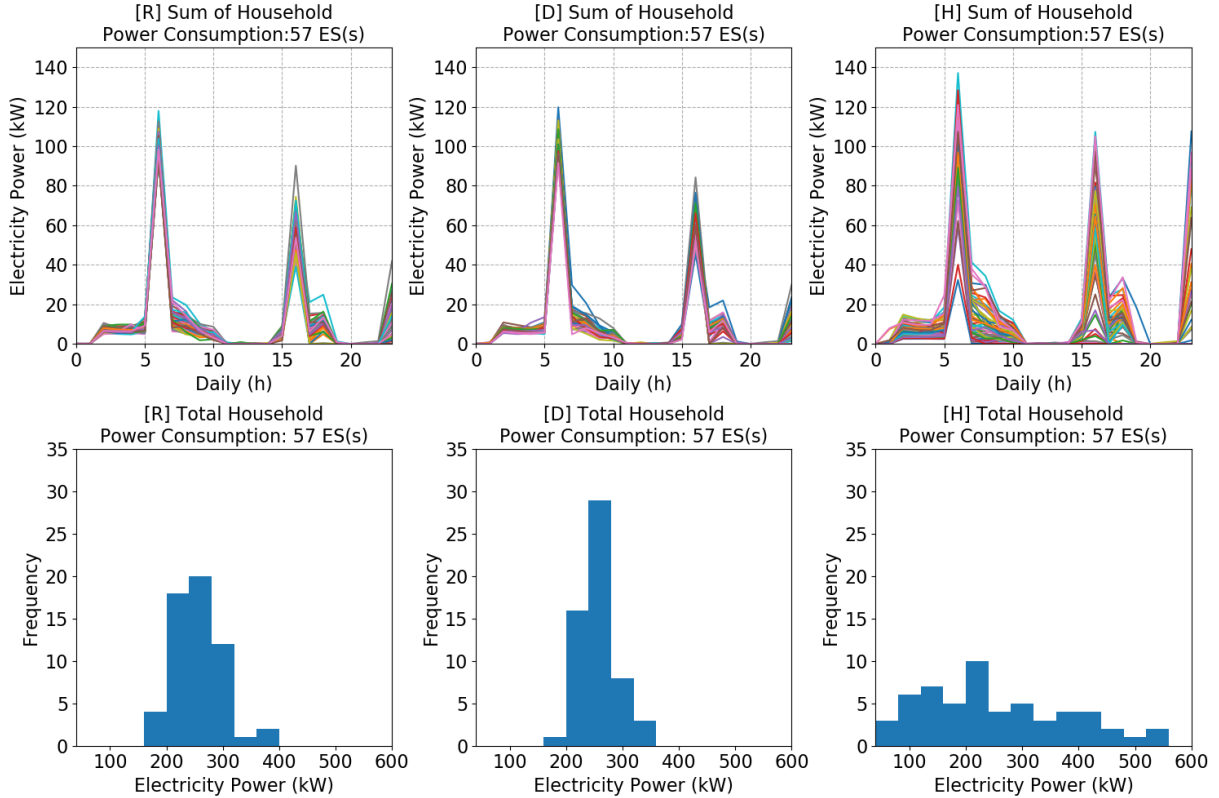


Figure 3.8: Comparing the households' load in each period and total households' load connected to the same CES for different CES allocation options in summer: [R] CES-random [D] CES-diverse [H] CES-homogeneous.

Moreover, when the per household utilization of energy storage is considered, the households charge/discharge less often when installing CESs than installing PES. The utilization for each household is calculated as (3.4), which considers the time of using energy storage

whether charging or discharging in period T .

$$\text{Per Household Utilization} = \frac{\sum_{t=0}^{|T|-1} s_{r,e,t}^{ch} + \sum_{t=0}^{|T|-1} s_{r,e,t}^{dis}}{|T|} \times 100\% \quad (3.4)$$

Figure 3.9 indicates the histogram of utilization for 1024 households where 57 CESs each of size 160kWh are allocated with different allocation options. When the households choose CES, the average utilization rate is around 44.15% to 45.13%, which means that the households usually spend 10.6 to 10.83 hours to charge or discharge power to save costs. In contrast, the average utilization rate rises to 49.67% if 1024 households use PES-single option, meaning that the households have to spend more time to achieve the same operational cost. The right-bottom of Figure 3.9 shows that most households have higher utilization which is above 50%.

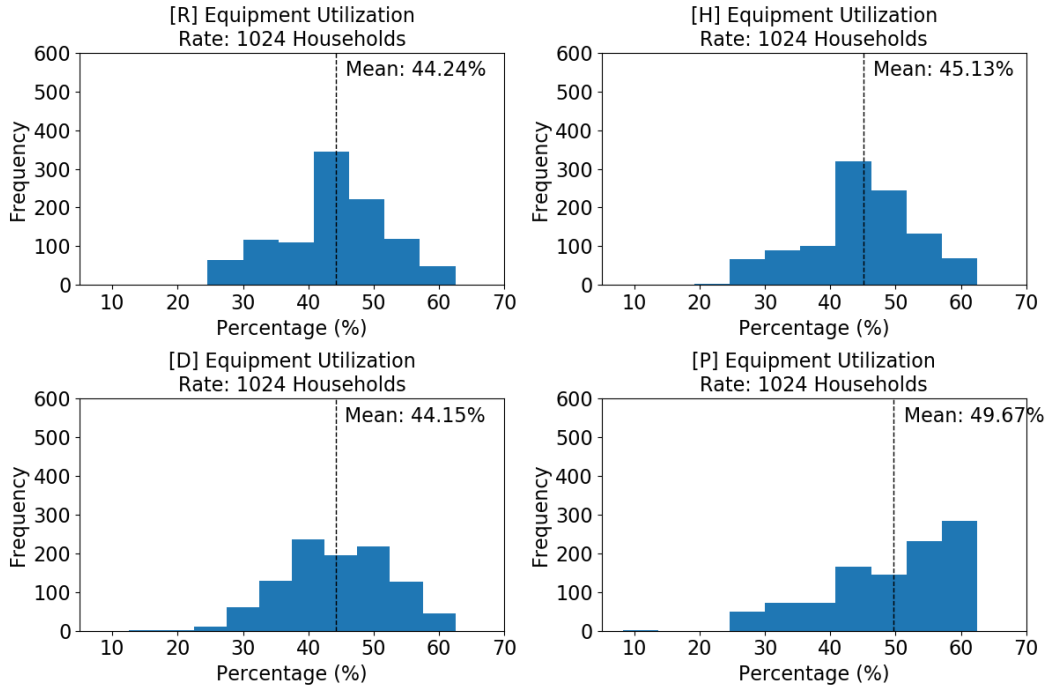


Figure 3.9: Comparing per household utilization rate of the energy storage among different allocation options in the summer day: [R] CES-random [D] CES-diverse [H] CES-homogeneous [P] PES-single.

Specifically, Figure 3.10 represents the time spent charging and discharging by households. It shows that some households spend more time either charging or discharging when they use PES-single option, and that is the reason why the average utilization rate is higher. In contrast, the overall frequency of charging and discharging is similar among the various CES options. This has a significant impact on the life cycle of the battery and thus the CES will have a better life span than the PES due to the amount of charging and discharging.

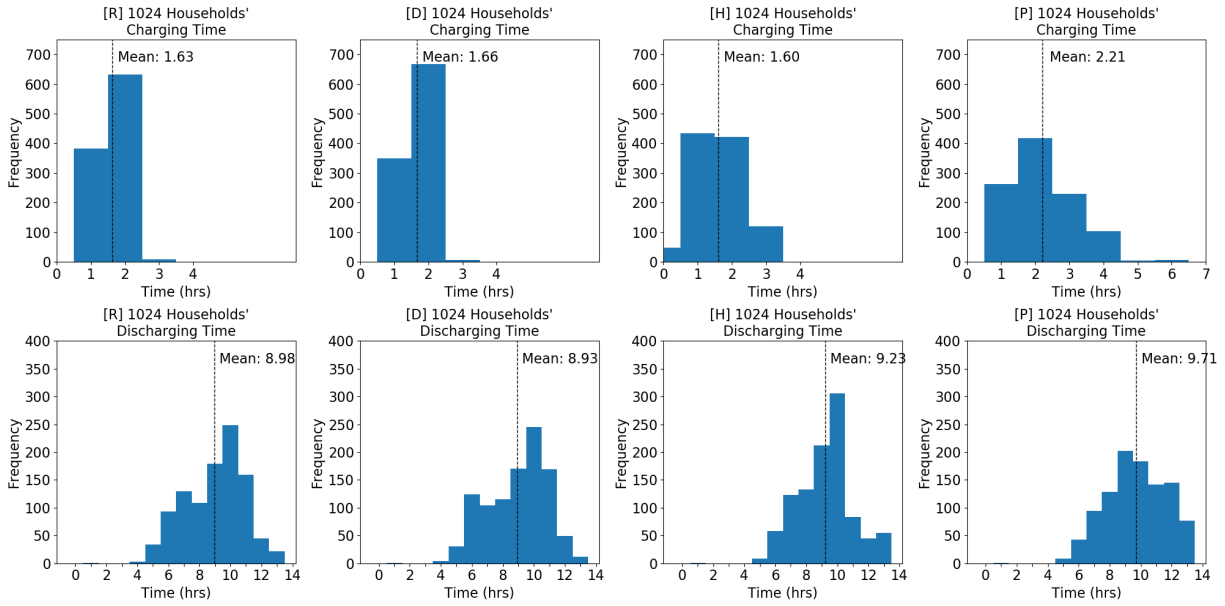


Figure 3.10: Comparing charging and discharging times of households among different allocation options in the summer day: [R] CES-random [D] CES-diverse [H] CES-homogeneous [P] PES-single.

Furthermore, when considering the overall utilization of CESs (as given in (3.5)), the CES-homogeneous option has more variations on the time of charging and discharging, see Figure 3.11. This is due to the consumption profiles of the households connected to the same CES as in this case some CESs need to be used more frequently to satisfy the demand of the households with high loads, and some CESs are not used frequently since the households have a lower load.

$$\text{Overall Utilization} = \frac{\sum_{r \in R_e} \sum_{t=0}^{|T|-1} s_{r,e,t}^{ch} + \sum_{r \in R_e} \sum_{t=0}^{|T|-1} s_{r,e,t}^{dis}}{|R_e| \times |T|} \times 100\% \quad (3.5)$$

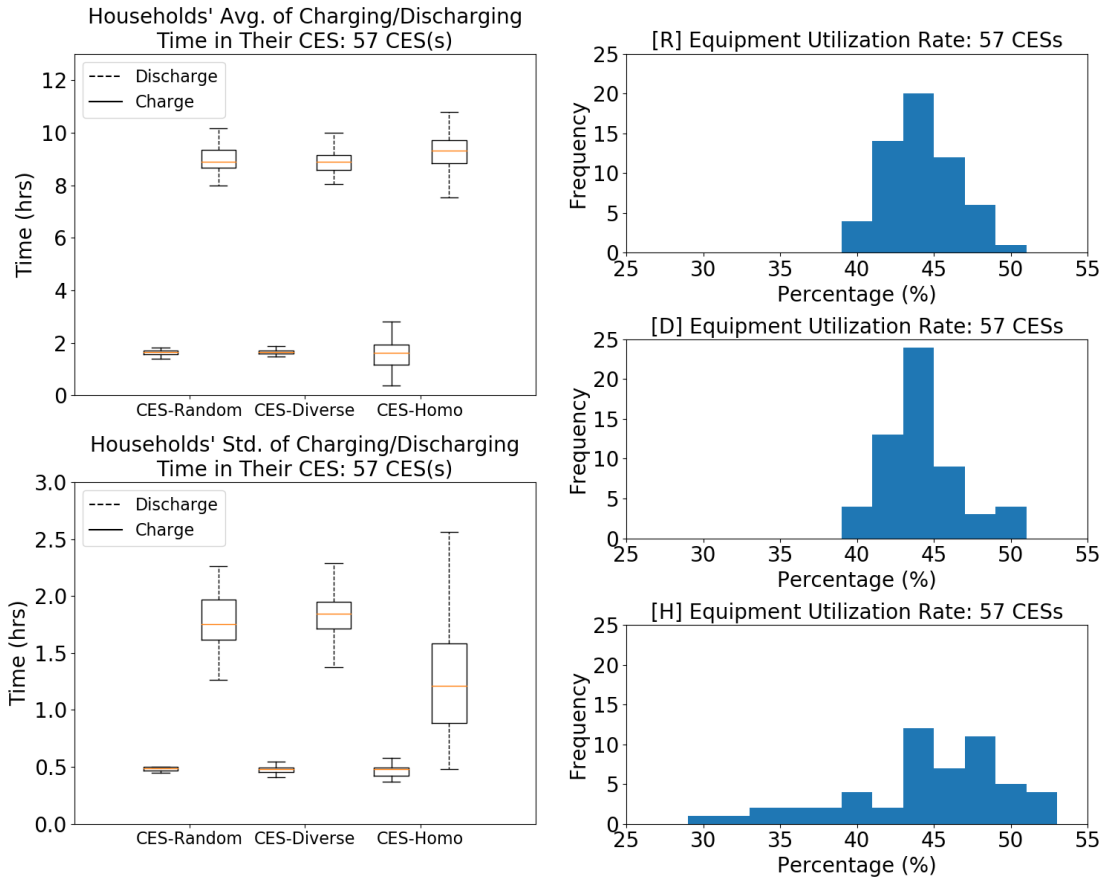


Figure 3.11: Comparing overall utilization rate of CESs among different CES allocation options in the summer day: [R] CES-random [D] CES-diverse [H] CES-homogeneous.

Finally, considering the households' behavior that are connected to the same CES, though CES-homogeneous option have more variations, it has better fairness than the other options. Figure 3.12 indicates the histogram using the same example above, which

compares the three different options using the average and the standard deviation of the ratio of charging and discharging for households connected to the same CES. The index is calculated as 3.6:

$$\Omega_r = \frac{\sum_{t=0}^{|T|-1} S_{r,e,t}^{ch}}{\sum_{t=0}^{|T|-1} S_{r,e,t}^{dis}} \quad (3.6)$$

The CES-random option and the CES-diverse option have larger average and standard deviation, meaning that the households do not fairly charge/discharge. In one CES, some households have significantly higher ratio than the others, which means they provide power for the others. In contrast, the CES-homogeneous option have lower average and standard deviation, it implies that all households in one CES fairly charge/discharge. Moreover, Figure 3.12 also provides the charging/discharging ratio Ω_r of all 1024 households. If the households select CES-homogeneous option, the ratio has frequencies close to 1, which it is more fair. In contrast, the CES-random option and the CES-diverse option have more outliers and the ratio is sometimes greater than 4.

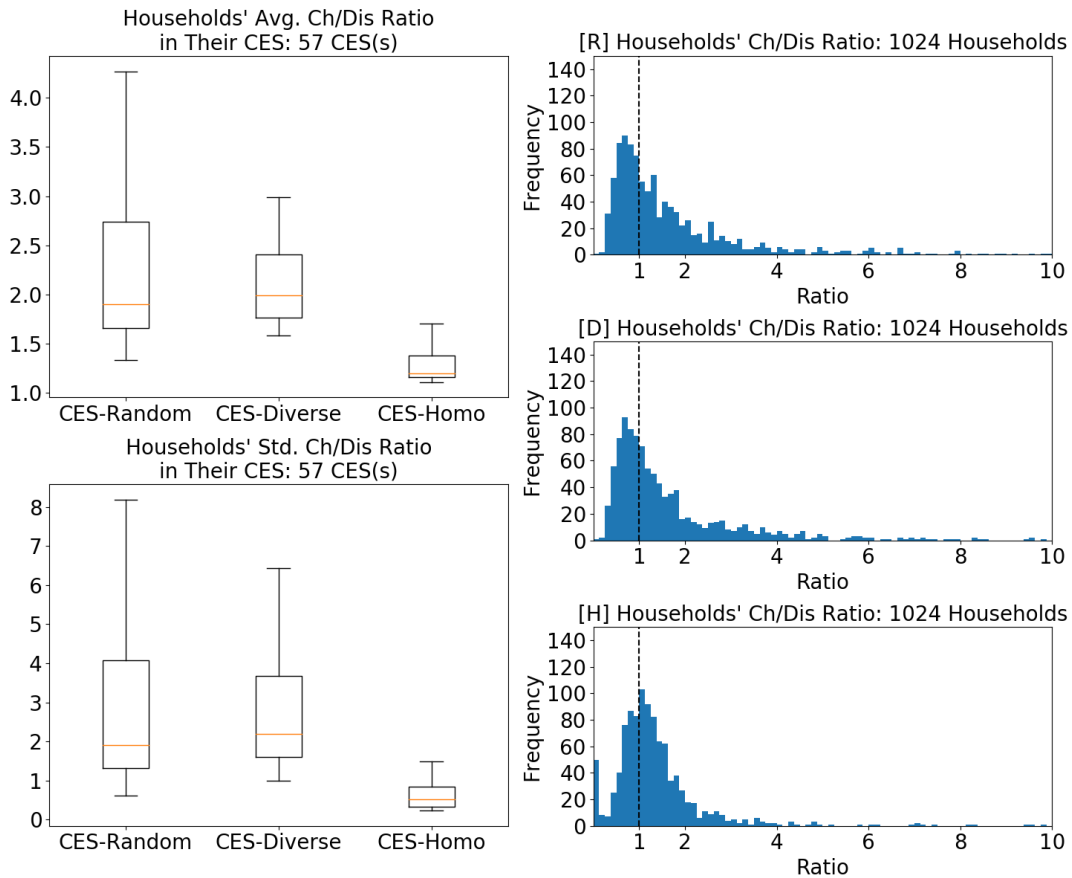


Figure 3.12: Fairness comparison for different CES allocation options in the summer day: [R] CES-random [D] CES-diverse [H] CES-homogeneous.

In summary, when households in Ennis connect to CES, some households would charge the CES while other households use this stored energy to minimize the overall costs. It has advantages that the households can share the power if they do not urgently need to consume that power when the energy price is high. For example, when the residents are not at home in a particular day, the power consumption of that household would be low, and the surplus of the generated power from the PV system of this household can be stored to the CES and used by the community neighbors. However, the fairness of utilizing the community energy storage system should be considered, in other words, it might cause problems if the ratio of charging and discharging is not satisfactory in a given community, causing some households to always to donate power to other households.

3.2 Case 2: Waterloo, Canada

For the second use case, a region in Canada is examined to simulate the results. The region is located in Waterloo, Ontario, Canada. The area contains 1133 households and the farthest physical distance between two households is 1.2 kilometers, which is suitable for installing CES.

3.2.1 Parameter Setting

The parameters are given according to the record in August 6, 2018, which is a typical summer day, and December 16, 2018, a common winter day without snow in Waterloo, Ontario, Canada. The parameters are displayed in Table 3.5.

The simulation period is one day, which sets $\Delta_T = 1$, $|T| = 24$. Also, Π_t is from Hourly Ontario Energy Price [43], see Figure 3.13. For the aggregator, the capacity of power consumption is assumed $A^{\min} = 0$ kW, $A^{\max} = 7.5 \text{ kW} \times 1133$ households, and $H_r^{\min} = 0$ kW and $H_r^{\max} = 15$ kW for each household.

The provincial load $U_{d,t}^{avg}$ is taken from IESO [44], which multiplies the proportion of households by the overall daily power consumption in Ontario, see Figure 3.13. Also, the home appliances categorized as uninterruptible load assume that the households use the same devices with ENERGY STAR certification in Canada in 2017 [45]. A dish washer would operate 2 hours with 1.2 kW in each hour. Also, a clothes washer would consume 0.75 kW and a clothes dryer operates 1.65 kW in an hour. Based on the information above, L and $\tilde{I}_{d,t}$ can be determined.

Moreover, considering the Canadians' life habits [46], the thermal load assumes the indoor temperature setting of HVAC Θ_t^{set} is in the range [20, 24] °C in summer and [18, 21] °C in winter. The ambient temperature record $\Theta_{d,t}^{avg}$ is taken from timeanddate.com, see Figure 3.13. For each air conditioner and space heating, the capacity of power consumption is considered as $\theta_d^{\min} = 0$ kW and $\theta_d^{\max} = 5$ kW. Based on thermodynamic model, thermal capacitance $C_d = 2.5$ kWh/°C, thermal resistance $R_d = 2$ °C/kW, and the working efficiency factor of HVAC $\eta_d = 2.5$ [9]. The degree tolerance is assumed to take a value of $\gamma = 2$ °C.

The PV system consists of a rooftop solar panel, which considers the specification of Canadian Solar CS6U-340P PV modules with nominal operating cell temperature (NOCT) mode, and assumes that each household installs 8 panels when it owns the PV system. $C_{d,t}^{avg}$

is taken from IESO, which refers to the daily record of Grand Renewable Energy Park, Ontario [47], see Figure 3.13.

The parameters of PES are according to the specification of Tesla Powerwall [41]. The battery state of charge is $B_e^{\max} = 13.5$ kWh and $B_e^{\min} = 0$ kWh. Efficiencies of charging and discharging are $\eta^{ch} = 0.948$ and $\eta^{dis} = 0.948$, yielding a 90% round-trip efficiency. The power capacity of PES is $S_e^{ch.\max} = S_e^{dis.\max} = 5$ kW and $S_e^{ch.\min} = S_e^{dis.\min} = 0$ kW.

Similarly, the parameters of CES refer to the specification of eCamion Community Energy Storage [42]. The battery capacity is $B_e^{\max} = 250$ kWh and $B_e^{\min} = 0$ kWh; the power capacity from households is $S_{r,e}^{ch.\max} = S_{r,e}^{dis.\max} = 5$ kW and $S_{r,e}^{ch.\min} = S_{r,e}^{dis.\min} = 0$ kW. The rated continuous power capacity of CES is $S_e^{ch.\max} = S_e^{dis.\max} = 500$ kW and $S_e^{ch.\min} = S_e^{dis.\min} = 0$ kW, and efficiencies of charging and discharging are formed $\eta^{ch} = 0.948$ and $\eta^{dis} = 0.948$, yielding a 90% round-trip efficiency as well.

Finally, the initial battery status $B_{e,-1}$ and the end battery status $B_{e,23}$ are assumed to be 40% of the maximum battery state of charge. B_e^{\max} for CES would be an important factor for the analysis, which means the maximum battery state of charge will vary when the analyzing the results.

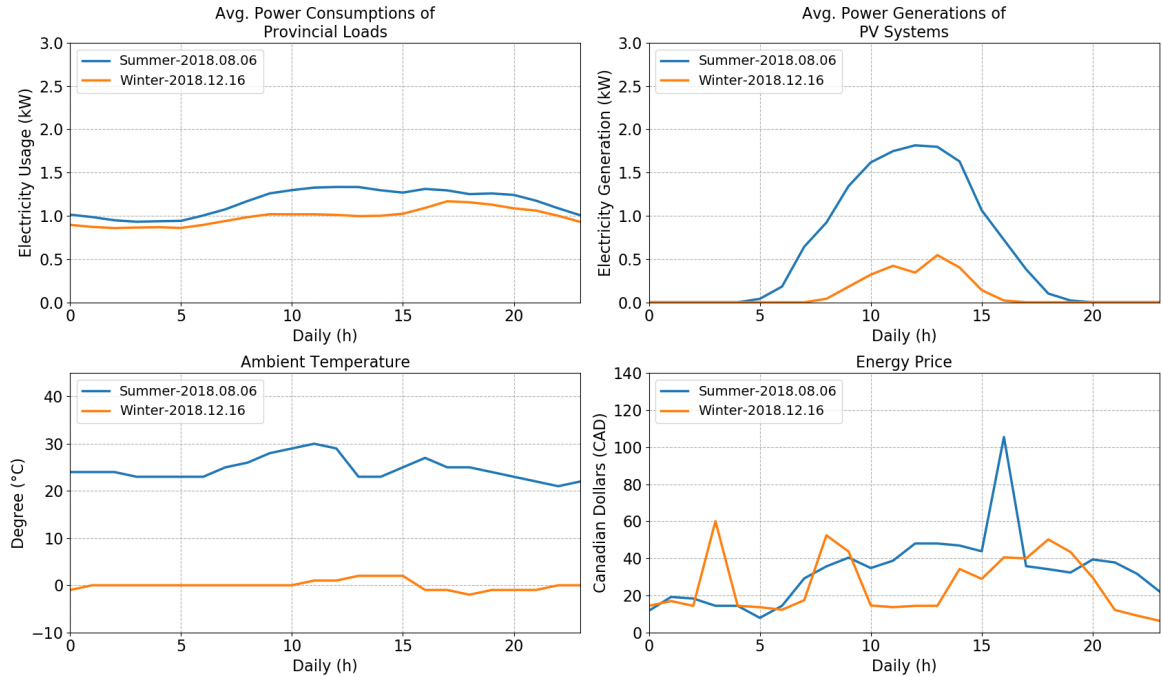


Figure 3.13: Daily charts for the parameters in Waterloo.

Table 3.5: Parameters of home appliances in Waterloo, Canada

Category	Parameters	Data Resource, Assumptions
Period time	$\Delta_T = 1, T = 24$	Simulating one day
Energy price	Π_t	IESO, Hourly Ontario Energy Price
Aggregator	$A^{\min} = 0, A^{\max} = 7.5 \times 1133$	
Household	$H_r^{\min} = 0, H_r^{\max} = 15$	
Provincial load	$U_{d,t}^{avg}$	IESO, zonal demand in Ontario
Dish washer	$\tilde{I}_{d,t} = [1.2, 1.2]$	BC Hydro, EnergyStar 2017, 2 hours
Clothes washer	$\tilde{I}_{d,t} = [0.75]$	BC Hydro, EnergyStar 2017, 1 hour
Clothes dryer	$\tilde{I}_{d,t} = [1.65]$	BC Hydro, EnergyStar 2017, 1 hour
Indoor temp. setting	$\Theta_t^{set} = [20, 24]$	Summer, Statistics Canada, HES 2015
Indoor temp. setting	$\Theta_t^{set} = [18, 21]$	Winter, Statistics Canada, HES 2015
Ambient temp.	$\Theta_{d,t}^{avg}$	timeanddate.com
AC or Heating	$\theta_d^{\min} = 0, \theta_d^{\max} = 3.5, \gamma = 2$ $C_d = 2.5, R_d = 2, \eta_d = 2.5$	
PV system	$C_{d,t}^{avg}$	IESO, Grand Renewable Energy Park, Ontario Canadian Solar CS6U-340P PV modules, 8 pcs
PES battery	$B_e^{\max} = 13.5, B_e^{\min} = 0$	Tesla Powerwall
PES efficiency	$\eta^{ch} = 0.948, \eta^{dis} = 0.948$	Tesla Powerwall
PES charging	$S_e^{ch, \max} = 5, S_e^{ch, \min} = 0$	Tesla Powerwall
PES discharging	$S_e^{dis, \max} = 5, S_e^{dis, \min} = 0$	Tesla Powerwall
CES battery	$B_e^{\max} = 250, B_e^{\min} = 0$	eCamion Community Energy Storage
CES efficiency	$\eta^{ch} = 0.948, \eta^{dis} = 0.948$	eCamion Community Energy Storage
CES charging	$S_e^{ch, \max} = 500, S_e^{ch, \min} = 0$	eCamion Community Energy Storage
CES discharging	$S_e^{dis, \max} = 500, S_e^{dis, \min} = 0$	eCamion Community Energy Storage
CES charging	$S_{r,e}^{ch, \max} = 5, S_{r,e}^{ch, \min} = 0$	eCamion Community Energy Storage
CES discharging	$S_{r,e}^{dis, \max} = 5, S_{r,e}^{dis, \min} = 0$	eCamion Community Energy Storage
Initial battery SOC	$B_{e,-1} = 40\%$	
Final battery SOC	$B_{e,23} = 40\%$	

Compared to case 1, residents' life habits are different in Canada as people consume more power in summer than in winter. In summer, people usually turn on the air conditioner to maintain indoor temperature. Also, the cycle time of uninterruptible load is shorter which is around one hour instead of four hours to complete the cycle. Finally, the energy price of the selected days fluctuate dramatically in a short period.

Secondly, the ownership rates of home appliances for the households are displayed in Table 3.6. The ownership rates of dish washer, clothes washer, clothes dryer refer to percentage of households as given by Statistics Canada [48], and the ownership rate of air conditioner and hydro space heating are taken from Households and the Environment

Survey [46].

Table 3.6: Ownership rates of home appliances in Waterloo, Canada

Devices	Category	Ownership rate
Dish washer	Uninterruptible load	60%
Clothes washer	Uninterruptible load	87%
Clothes dryer	Uninterruptible load	83%
Air conditioner	Thermal load	57%
Hydro space heating	Thermal load	11%
Rooftop solar	PV system	0% - 100%
PES or CES	Energy storage	0% - 100%
Others	Provincial load	100%

3.2.2 Community Setting

The communities are built by using k -mean approach based on their longitude and latitude. In this case, similar to the previous one, $K = 3$ is used to form three communities, and the size of these communities are 337, 572, and 224 households respectively, see Figure 3.14.

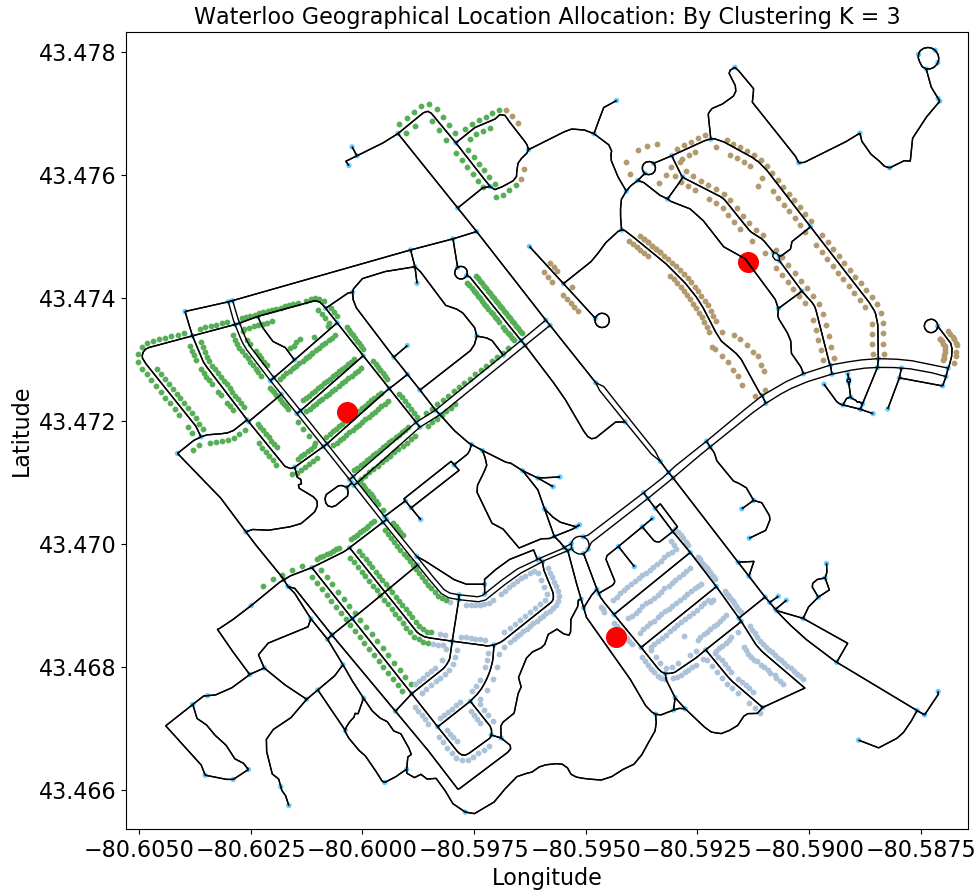


Figure 3.14: Region map and households' locations in Waterloo, Canada.

3.2.3 Computational Results

3.2.3.1 Features for PES

Figure 3.15 indicates the heat-map of the operational cost when the ownership rate of PV system and PES increase. Compared to case 1, the operational cost in Waterloo reduces more but the trend is the same, meaning that PV systems can help households reduce their costs significantly during the summer, and energy storage can provide a stable cost

reduction for the households whether in the summer or winter.

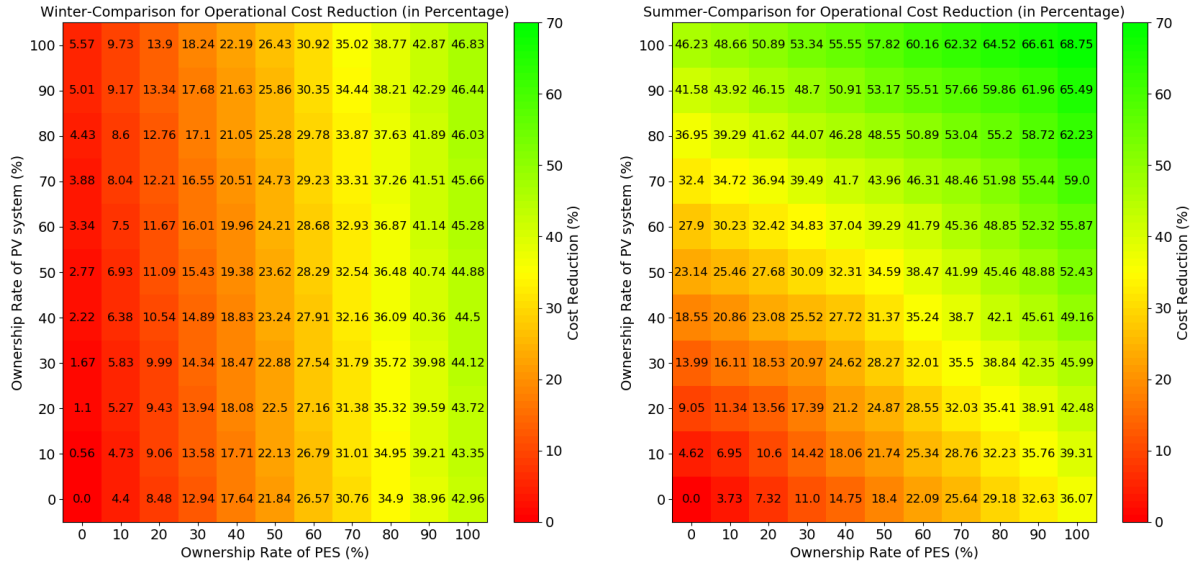


Figure 3.15: Operational cost reduction varying the ownership rate of PV system and PES in Waterloo.

Moreover, the charging and discharging ratio Ω is still the same for all the households, which is 1.113 as it is only related to the specification of PES system, which is its charging and discharging efficiency, see Figure 3.16. Though the energy price fluctuates more for this use case, the households' charging and discharging pattern follow a similar behavior that is they charge the PES when the energy price is low and discharge when the price is high.

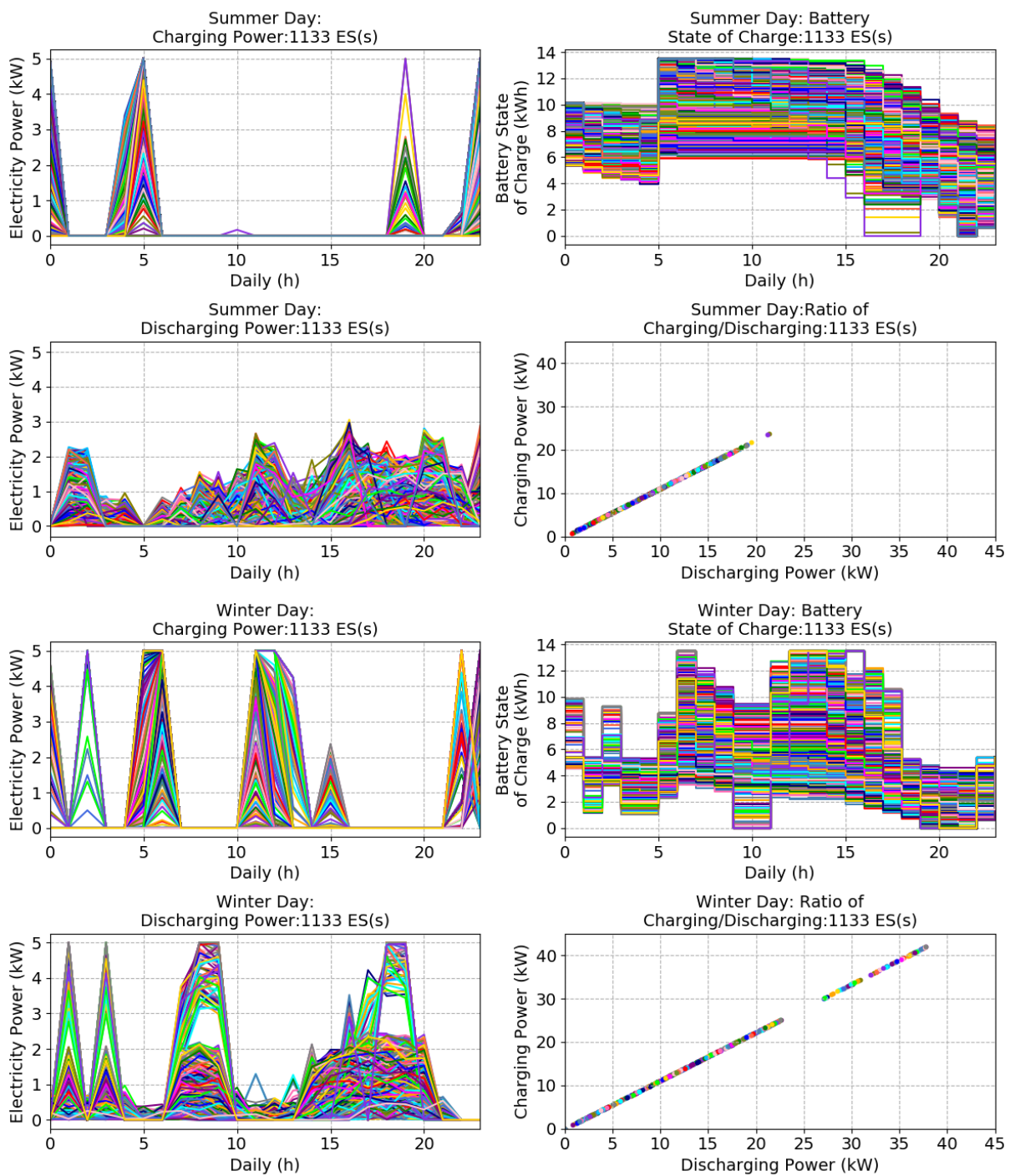


Figure 3.16: Features for charging and discharging of PES.

3.2.3.2 Determining Battery Capacity of CES

Compared to case 1, the number of households and the size of communities are slightly bigger. Assuming all the households connect to one CES and own a PV system, the range of average battery capacity for each household to have a lower operational cost than PES is within [8.261, 13.5] and [9.885, 13.5] for the winter day and summer day, respectively considering a random allocation. Compared with case 1, the power generation of these regions is similar but the power consumption is quite different, and also, the energy price is more fluctuating in Waterloo. Additionally, diminishing marginal utility still exists in this case, see Figure 3.17.

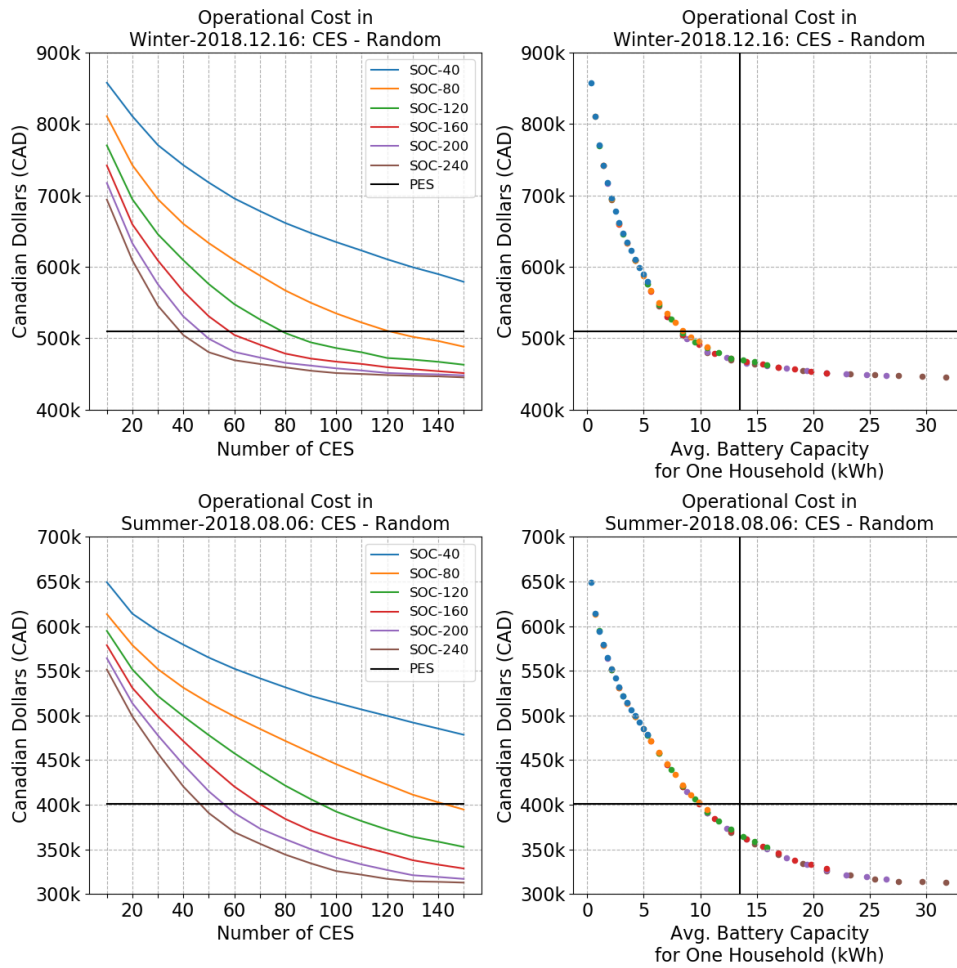


Figure 3.17: Operational cost varying battery capacity and number of CES.

3.2.3.3 Allocation Options for CES

Figure 3.18 compares the operation cost among three allocation methods: CES-random, CES-diverse, and CES-homogeneous when the average battery capacity for each household increases. The result shows the same patterns as case 1 that the optimal costs have no significant difference between CES-random and CES-diverse, but the cost of CES-homogeneous is higher.

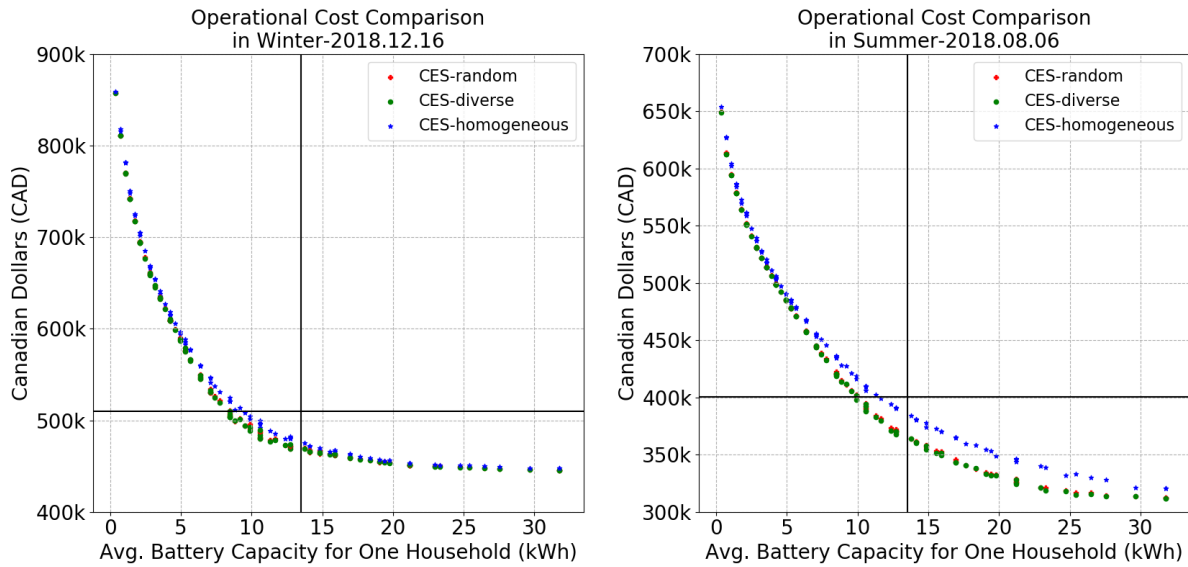


Figure 3.18: Operational cost for different CES allocation options.

Additionally, Figure 3.19 provides the charging, discharging, state of charge, and ratio of charging vs. discharging patterns for the community with 71 CESs each of size 160 kWh in the summer day, and Figure 3.20 shows the summation of household net load in each period and total household net load. Compared to case 1, the schedule of charging, discharging, and battery state of charge changes based on the power consumption, power generation and energy price, however, the behaviors are similar in the sense that the households select to charge the CES when the energy price is low and discharge from CES when the energy price is high, it implies that the energy price influences the schedule of CES significantly in these two cases. Also, the CES-diverse and CES-homogeneous options perform the same patterns on the household net load in two use cases.

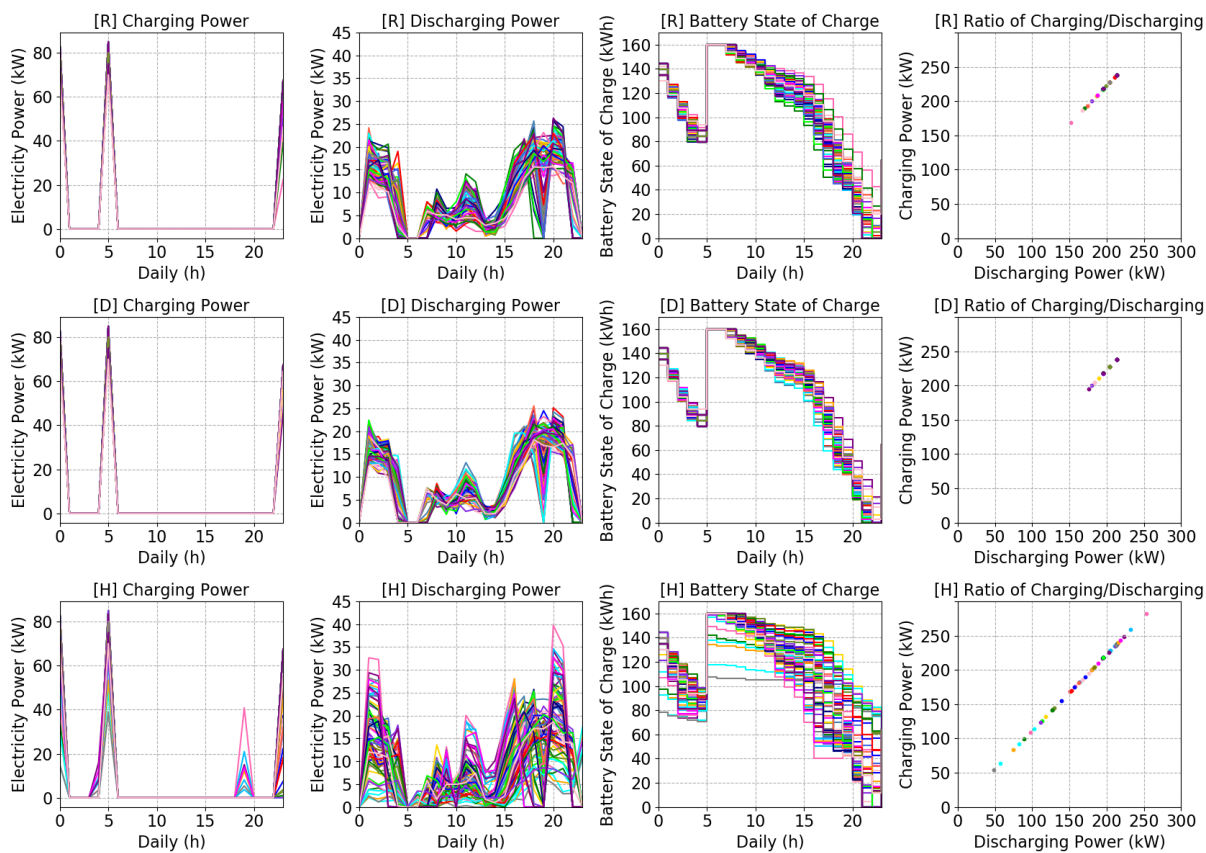


Figure 3.19: Comparing battery charging, discharging, state of charge, and ratio of charging vs discharging among different CES allocation options in summer: [R] CES-random [D] CES-diverse [H] CES-homogeneous.

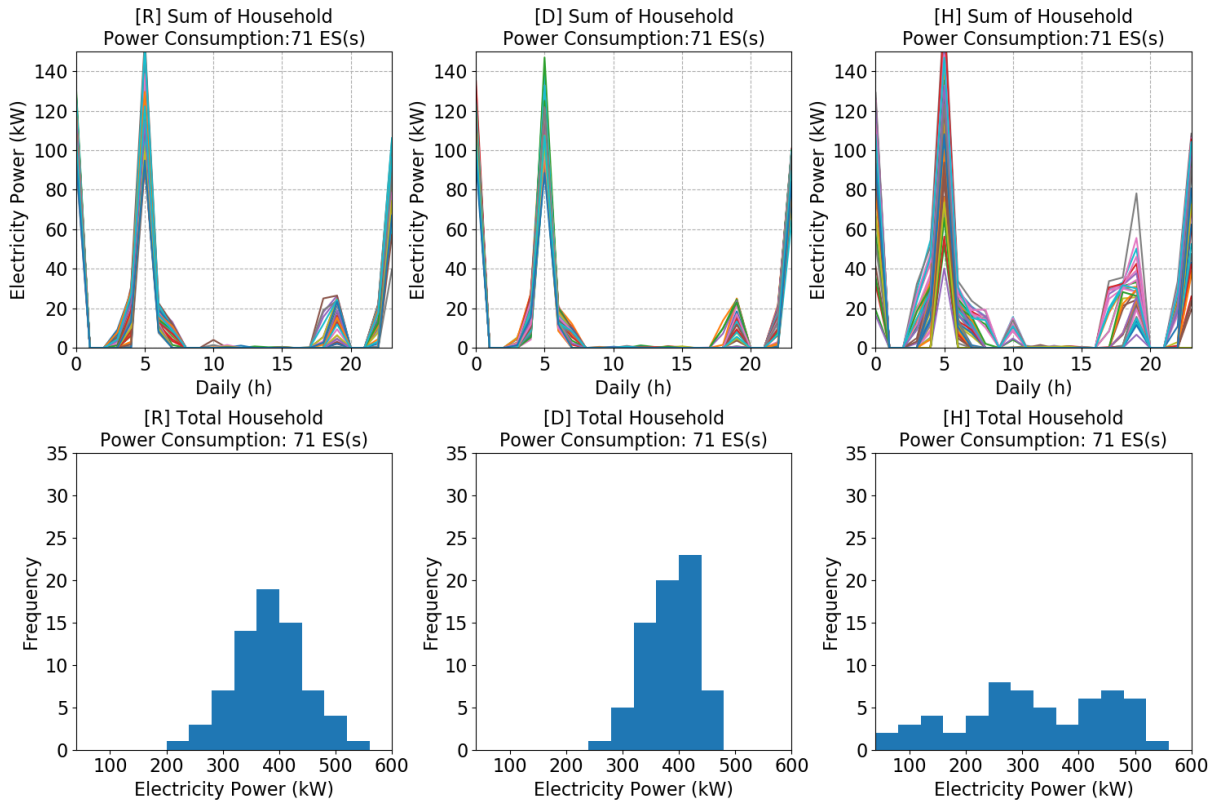


Figure 3.20: Comparing the households' load in each period and total households' load connected to the same CES for different CES allocation options in summer: [R] CES-random [D] CES-diverse [H] CES-homogeneous.

Moreover, Figure 3.21 indicates the histogram of the per household utilization for 1133 households where 71 CESs each of size 160kWh are allocated with different allocation options. When the households choose CES, the average utilization rate is around 65.55% to 67.38%. In contrast, the average utilization rate rises to 72.08% if households use PES-single option, which means the households have to spend more time charging and discharging, see the right-bottom of Figure 3.21. Such behavior impacts the battery performance and can degrade the battery relatively quickly.

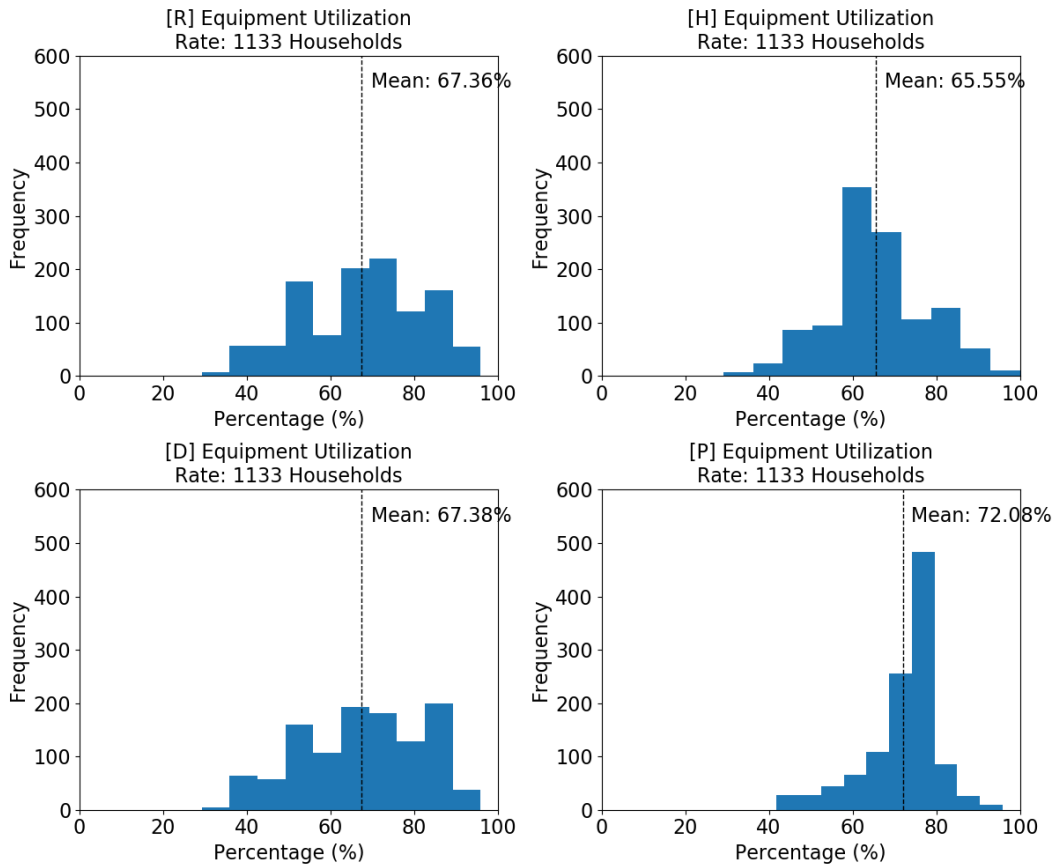


Figure 3.21: Comparing per household utilization rate of the energy storage among different allocation options in the summer day: [R] CES-random [D] CES-diverse [H] CES-homogeneous [P] PES-single.

Also, Figure 3.22 represents the time spent charging and discharging by households. It shows that some households spend more time either charging or discharging when they use PES-single option. The various CES options exhibit a similar behavior in this case as well. Compared to case 1, the pattern of the computational result is similar.

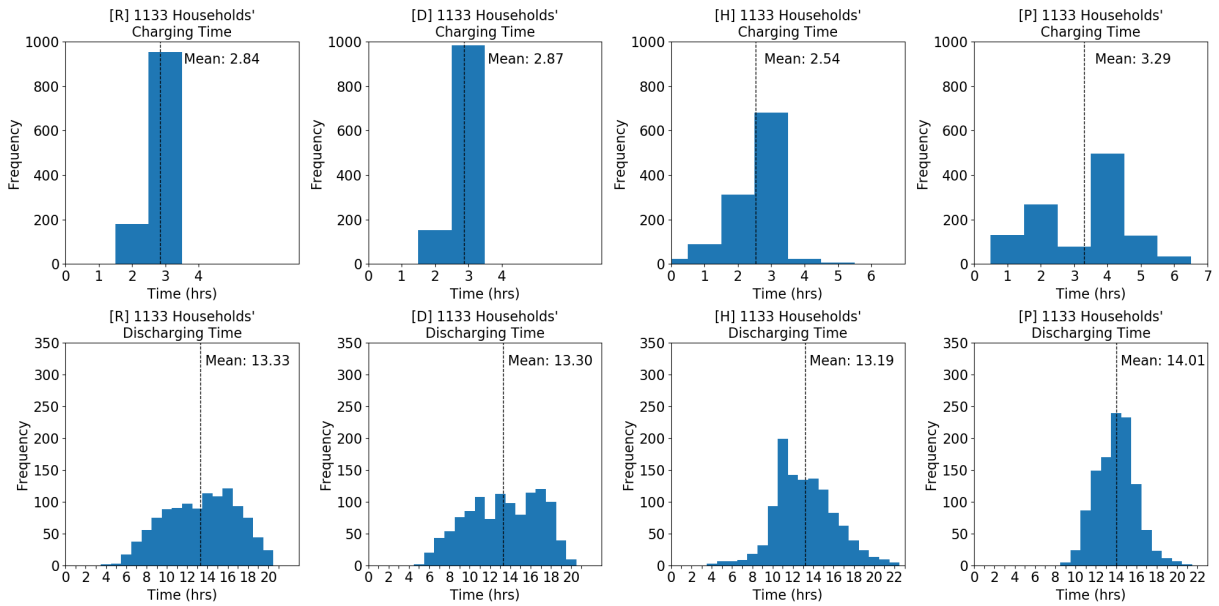


Figure 3.22: Comparing charging and discharging time of households among different allocation options in the summer day: [R] CES-random [D] CES-diverse [H] CES-homogeneous [P] PES-single.

Furthermore, when considering the overall utilization of CESs, it has similar trend as case 1, that is, the CES-homogeneous option has more variations on the time of charging and discharging as shown in Figure 3.23.

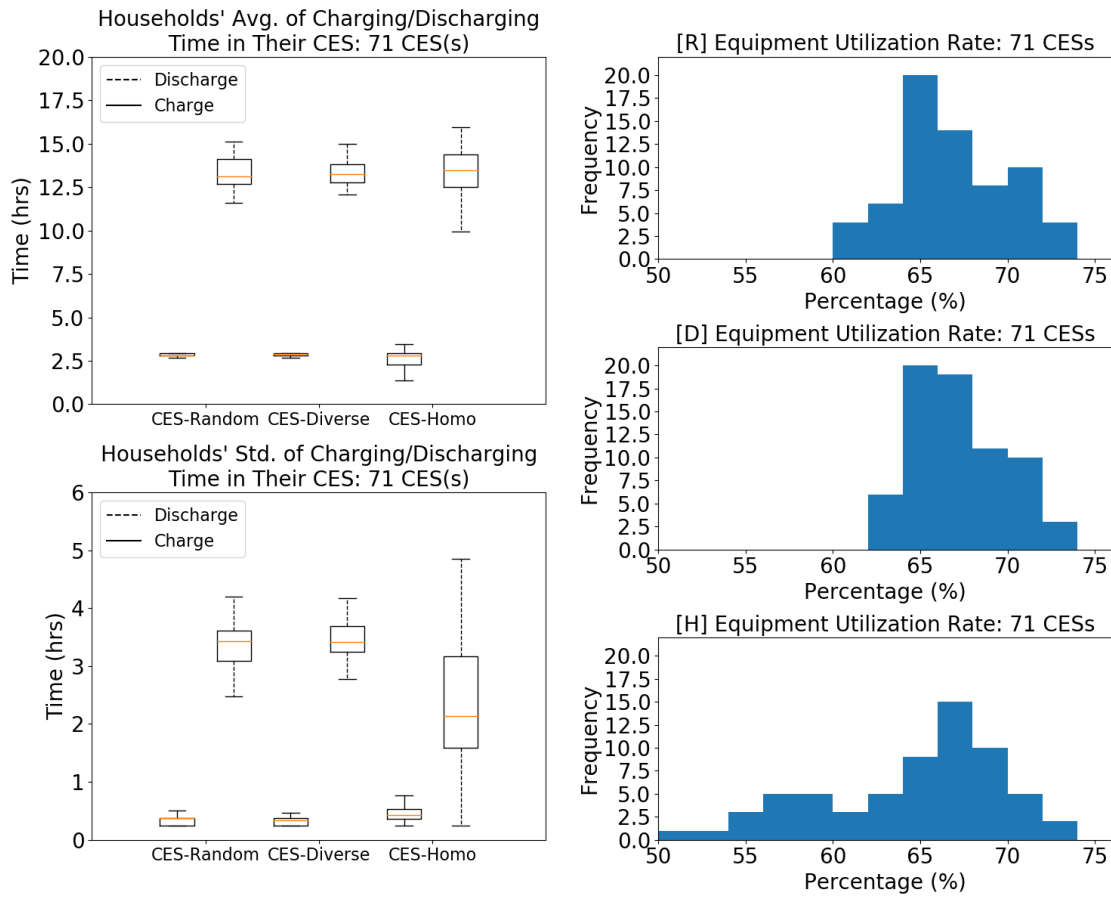


Figure 3.23: Comparing overall utilization rate of CESs among different CES allocation options in the summer day: [R] CES-random [D] CES-diverse [H] CES-homogeneous.

The three allocation options show similar trends as case 1, that is the CES-homogeneous option has better fairness, see Figure 3.24. The CES-homogeneous option has a lower average and standard deviation for the charging/discharging ratio where most of the values are close to 1 and very few outliers with values bigger than 4.

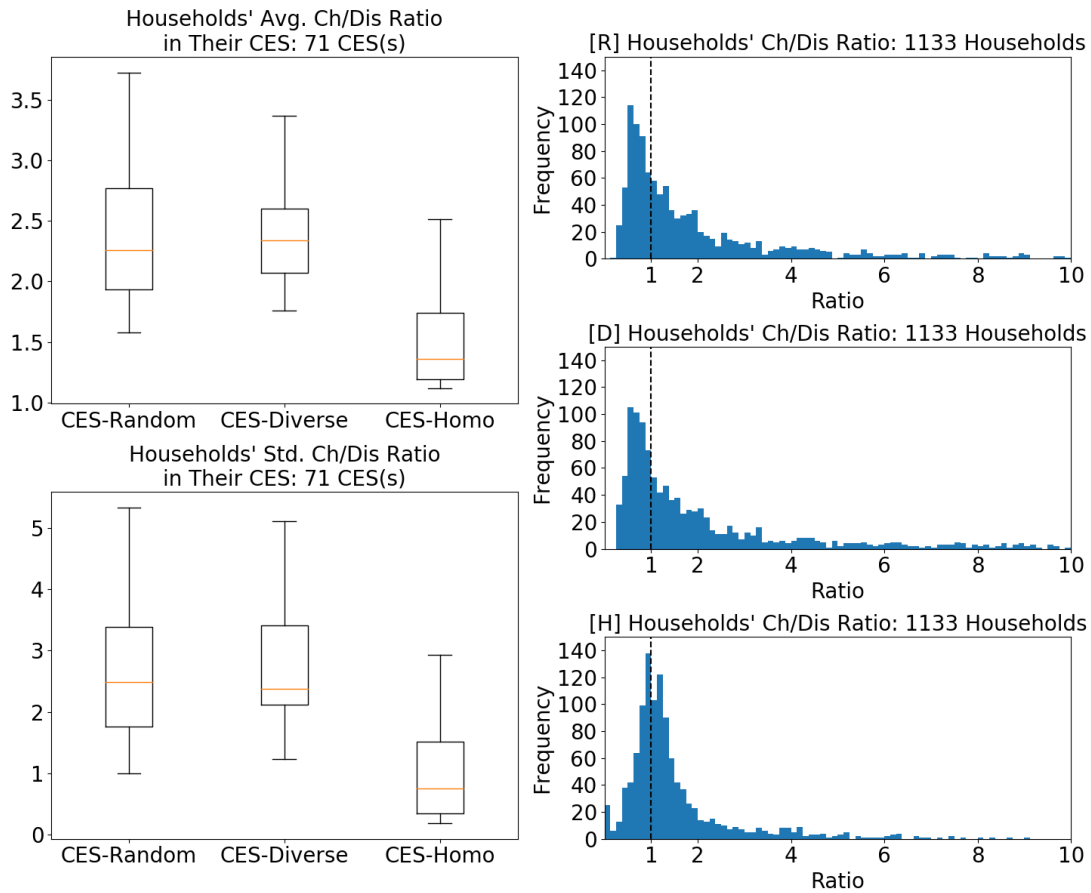


Figure 3.24: Fairness comparison for CES allocation options in the summer day: [R] CES-random [D] CES-diverse [H] CES-homogeneous.

In summary, the two cases show that the optimal battery capacity of CES changes based on households' power consumption behavior and the energy price in the region and the patterns of charging and discharging follow the energy price. Also, the overall cost reduction of installing CES is greater than installing PES for the households no matter what allocation option is used.

Chapter 4

Conclusion

4.1 Summary and Conclusion

This research develops a framework to effectively calculate the operational cost of a community which can be applied to any region with different number of devices, specification, residential habits, and allocation options. By using k -mean for allocating energy storage and formulating an MILP model, the analysis compares different scenarios, including different types of appliances, PV systems, energy storages, households power consumption profiles in an individual set-up as well as a community set-up. Also, the optimal schedule of home appliances and DERs for each household can be monitored graphically by using a software with a user interface that was implemented for such problems.

A number of conclusions and important observations resulting from the presented work can be made, and are summarized as follows:

- For the case of CES-diverse, the optimization model can be decomposed to the number of energy storage devices and each local community's operation can be optimized independently. In other words, the optimal cost for the aggregator would be equal to the summation of the optimal cost for each community independently.
- Households can have substantial cost reduction when they install energy storage and PV system. Considering PES, it can provide a stable cost reduction for the household, and PV system can help a household reduce its costs significantly in the summer day. The level of cost reduction varies based on the region, residential habits, energy price, etc.

- In the deterministic optimization model, the ratio of storing power and consuming power Ω is determined by the efficiencies of charging and discharging only, which is its round-trip efficiency.
- For the case of CES, the PV systems can provide the CESs with more flexibility to adjust the average battery capacity in the summer day. Also, since the marginal utility of the battery capacity is diminishing, the suitable average battery capacity for each household is determined in the range based on their life habits.
- Compared to PES option, the households in a community can have a lower costs as the capital cost and operational cost are lower when they select CES option.
- Given the same conditions of households, the operational costs of CES-diverse option are slightly lower than the cost of CES-random option, and the cost of CES-homogeneous option is higher than the others whether any region is. Also, the CES-diverse option causes the CESs to have almost the same patterns for charging, discharging and battery state of charge; the CES-homogeneous option have more different patterns. For the CES-random option, the patterns are between CES-diverse and CES-homogeneous.
- When the households choose CES, the average utilization rate is lower than PES-single option, meaning that the households charge/discharge less frequently which positively impacts the battery's life and maintenance costs.
- Considering the households' behavior that are connected to the same CES, although CES-homogeneous option have more variations, it has better fairness than the other options.

4.2 Future Work

The research provides useful insights and analysis for the deployment of shared DERs, however, there is still room for improvement.

First, the optimization model is built based on deterministic number of inputs, which means it does not consider uncertainty of the future. Therefore, the model may need to be improved considering a stochastic model or robust model to closely mimic the reality. For example, some factors causing uncertainty such as dynamic power generation from the PV system, energy prices, equipment performance in a dynamic basis, load variation, etc., could be considered into the model. Secondly, the battery size and number in this case is varied to take into account different options, however, for better results the battery number and size can be part of the optimization model as this would optimize the overall total costs. Additionally, the model considers one day for optimizing these cases, however, the one day simulation period might not enough to reflect the reality. Finally, the model does not consider the fairness of households as it only considers the rational scenario that all the households are willing to cooperate together. Fairness is always a big problem for such collaborative models, and the model needs to investigate and optimize this KPI further to make the households feel comfortable in such systems.

References

- [1] The Mowat Centre, “Background Report on the Ontario Energy Sector,” The Mowat Centre, Toronto, Tech. Rep., 2016. [Online]. Available: https://mowatcentre.ca/wp-content/uploads/publications/134_EET_background_report_on_the_ontario_energy-sector.pdf
- [2] The Independent Electricity System Operator (IESO), “Total Annual Ontario Energy Demand,” 2019. [Online]. Available: <http://www.ieso.ca/en/Power-Data/Demand-Overview/Historical-Demand>
- [3] Association of Power Producers Of Ontario (APPrO), “Toronto’s unique energy challenge,” 2015. [Online]. Available: <https://magazine.appro.org/news/ontario-news/3872-torontos-unique-energy-challenge-.html>
- [4] L. M. Camarinha-Matos, “Collaborative smart grids A survey on trends,” *Renewable and Sustainable Energy Reviews*, vol. 65, pp. 283–294, 2016.
- [5] V. C. Gungor, D. Sahin, T. Kocak, S. Ergut, C. Buccella, S. Member, C. Cecati, G. P. Hancke, and S. Member, “A Survey on Smart Grid Potential Applications and Communication Requirements,” *IEEE Transactions on Industrial Informatics*, vol. 9, no. 1, pp. 28–42, 2013.
- [6] V. Fthenakis, J. E. Mason, and K. Zweibel, “The technical, geographical, and economic feasibility for solar energy to supply the energy needs of the US,” *Energy Policy*, vol. 37, no. 2, pp. 387–399, 2009.
- [7] L. Gkatzikis, I. Koutsopoulos, and T. Salonidis, “The Role of Aggregators in Smart Grid Demand,” *IEEE Journal on Selected Areas in Communications*, vol. 31, no. 7, pp. 1247–1257, 2013.

- [8] M. C. Bozchalui, S. A. Hashmi, H. Hassen, C. A. Cañizares, and K. Bhattacharya, “Optimal operation of residential energy hubs in smart grids,” *IEEE Transactions on Smart Grid*, vol. 3, no. 4, pp. 1755–1766, 2012.
- [9] J. L. Mathieu, “Modeling, Analysis, and Control of Demand Response Resources,” Ph.D. dissertation, University of California, Berkeley, 2012.
- [10] M. Talha, M. S. Saeed, G. Mohiuddin, M. Ahmad, M. Nazar, and N. Javaid, “Energy Optimization in Home Energy Management System Using Artificial Fish Swarm Algorithm and Genetic Algorithm,” in *International Conference on Intelligent Networking and Collaborative Systems*, 2018, pp. 203–213.
- [11] W. Kong, Z. Y. Dong, D. J. Hill, F. Luo, and Y. Xu, “Short-Term Residential Load Forecasting Based on Resident Behaviour Learning,” *IEEE Transactions on Power Systems*, vol. 33, no. 1, pp. 1087–1088, 2018.
- [12] M. S. Ahmed, A. Mohamed, T. Khatib, H. Shareef, R. Z. Homod, and J. Abd, “Real time optimal schedule controller for home energy management system using new binary backtracking search algorithm,” *Energy & Buildings*, vol. 138, pp. 215–227, 2017.
- [13] N. G. Paterakis, O. Erdinç, A. G. Bakirtzis, and J. P. Catalão, “Optimal household appliances scheduling under day-ahead pricing and load-shaping demand response strategies,” *IEEE Transactions on Industrial Informatics*, vol. 11, no. 6, pp. 1509–1519, 2015.
- [14] I. Sharma, J. Dong, A. A. Malikopoulos, M. Street, J. Ostrowski, T. Kuruganti, and R. Jackson, “A modeling framework for optimal energy management of a residential building,” *Energy and Buildings*, vol. 130, pp. 55–63, 2016.
- [15] H. Pandžić, “Optimal battery energy storage investment in buildings,” *Energy and Buildings*, vol. 175, pp. 189–198, 2018.
- [16] O. M. Longe, K. Ouahada, S. Rimer, A. N. Harutyunyan, and H. C. Ferreira, “Distributed Demand Side Management with Battery Storage for Smart Home Energy Scheduling,” *Sustainability, MDPI, Open Access Journal*, vol. 9, no. 1, pp. 1–13, 2017.
- [17] S. Nan, M. Zhou, and G. Li, “Optimal residential community demand response scheduling in smart grid,” *Applied Energy*, vol. 210, pp. 1280–1289, 2018.
- [18] M. F. Anjos, A. Lodi, and M. Tanneau, “A decentralized framework for the optimal coordination of distributed energy resources,” *IEEE Transactions on Power Systems*, vol. 34, no. 1, pp. 1–8, 2019.

- [19] H. Alharbi and K. Bhattacharya, “Stochastic Optimal Planning of Battery Energy Storage Systems for Isolated Microgrids,” *IEEE Transactions on Sustainable Energy*, vol. 9, no. 1, pp. 211–227, 2018.
- [20] Y. Yang, S. Bremner, C. Menictas, and M. Kay, “Battery energy storage system size determination in renewable energy systems: A review,” *Renewable and Sustainable Energy Reviews*, vol. 91, no. April, pp. 109–125, 2018.
- [21] J. Sardi and N. Mithulanathan, “Community energy storage, a critical element in smart grid: A review of technology, prospect, challenges and opportunity,” in *2014 4th International Conference on Engineering Technology and Technopreneuship, ICE2T 2014*. Kuala Lumpur, Malaysia: IEEE, 2014, pp. 125–130.
- [22] B. P. Koirala, E. van Oost, and H. van der Windt, “Community energy storage: A responsible innovation towards a sustainable energy system?” *Applied Energy*, vol. 231, pp. 570–585, 2018.
- [23] J. Sardi, N. Mithulanathan, and D. Q. Hung, “Strategic allocation of community energy storage in a residential system with rooftop PV units,” *Applied Energy*, vol. 206, pp. 159–171, 2017.
- [24] J. Sardi, N. Mithulanathan, M. Gallagher, and D. Q. Hung, “Multiple community energy storage planning in distribution networks using a cost-benefit analysis,” *Applied Energy*, vol. 190, pp. 453–463, 2017.
- [25] D. Parra, M. Gillott, S. A. Norman, and G. S. Walker, “Optimum community energy storage system for PV energy time-shift q,” *Applied Energy*, vol. 137, pp. 576–587, 2015.
- [26] G. Ye, G. Li, D. I. Wu, X. Chen, and Y. Zhou, “Towards Cost Minimization With Renewable Energy Sharing in Cooperative Residential Communities,” *IEEE Access*, vol. 5, pp. 11 688 – 11 699, 2017.
- [27] C. Long, J. Wu, C. Zhang, M. Cheng, and A. Al-wakeel, “Feasibility of peer-to-peer energy trading in low voltage electrical distribution networks,” in *8th International Conference on Applied Energy, ICAE 2016*, vol. 105. Beijing, China: Elsevier, 2017, pp. 2227–2232.
- [28] A. Anvari-moghaddam, A. Rahimi-kian, M. S. Mirian, and J. M. Guerrero, “A multi-agent based energy management solution for integrated buildings and microgrid system,” *Applied Energy*, vol. 203, pp. 41–56, 2017.

- [29] D. Mahmood, N. Javaid, I. Ahmed, N. Alrajeh, I. A. Niaz, and Z. A. Khan, “Multi-agent-based sharing power economy for a smart community,” *International Journal of Energy Research*, vol. 41, no. 14, pp. 2074–2090, 2017.
- [30] W. Tushar, B. Chai, C. Yuen, S. Huang, D. B. Smith, H. V. Poor, and Z. Yang, “Energy Storage Sharing in Smart Grid : A Modified Auction-Based Approach,” *IEEE Transactions on Smart Grid*, vol. 7, no. 3, pp. 1462–1475, 2016.
- [31] J. Rajasekharan and V. Koivunen, “Cooperative Game-theoretic Approach to Load Balancing in Smart Grids with Community Energy Storage,” in *2015 23rd European Signal Processing Conference, EUSIPCO 2015*. Nice, France: IEEE, 2015, pp. 1955 – 1959.
- [32] E. Barbour, D. Parra, Z. Awwad, and M. C. González, “Community energy storage : A smart choice for the smart grid ?” *Applied Energy*, vol. 212, pp. 489–497, 2018.
- [33] S. V. D. Stelt, T. Alskaf, and W. V. Sark, “Techno-economic analysis of household and community energy storage for residential prosumers with smart appliances,” *Applied Energy*, vol. 209, pp. 266–276, 2018.
- [34] I. S. Bayram, M. Abdallah, A. Tajer, and K. A. Qaraqe, “A Stochastic Sizing Approach for Sharing-Based Energy Storage Applications,” *IEEE Transactions on Smart Grid*, vol. 8, no. 3, pp. 1075–1084, 2017.
- [35] F. Hafiz, A. R. de Queiroz, P. Fajri, and I. Husain, “Energy management and optimal storage sizing for a shared community : A multi-stage stochastic programming approach,” *Applied Energy*, vol. 236, pp. 42–54, 2019.
- [36] Sustainable Energy Authority of Ireland, “Energy in the Residential Sector 2018 Report,” Sustainable Energy Authority of Ireland, Dublin, Tech. Rep., 2018. [Online]. Available: <https://www.seai.ie/resources/publications/Energy-in-the-Residential-Sector-2018-Final.pdf>
- [37] M. Jakubcionis and J. Carlsson, “Estimation of European Union residential sector space cooling potential,” *Energy Policy*, vol. 101, pp. 225–235, 2017.
- [38] Nord Pool AS, “N2EX Day Ahead Auction Prices,” 2018. [Online]. Available: <https://www.nordpoolgroup.com/Market-data1/GB/Auction-prices/UK/Hourly/?view=table>

- [39] The Commission for Energy Regulation, “Electricity Smart Metering Technology Trials Findings Report,” The Commission for Energy Regulation, Dublin, Tech. Rep., 2011. [Online]. Available: <https://www.ucd.ie/issda/t4media/ElectricitySmartMeteringTechnologyTrialsFindingsReport.pdf>
- [40] Activ8 Solar Energies, “Solar PV 56 kWp System Installed in Courtown Co. Wexford,” 2018. [Online]. Available: <https://activ8energies.com/solar-pv-56-kwp/>
- [41] Tesla, “Tesla Powerwall 2 Datasheet - North America,” 2018. [Online]. Available: https://www.tesla.com/sites/default/files/pdfs/powerwall/Powerwall2_AC_Datasheet_en_northamerica.pdf
- [42] eCAMION Inc., “250kWh Community Energy Storage System Specification,” 2013. [Online]. Available: https://www.ecamion.com/images/brochures/8_eCamion_CommunityEnergyStorage.pdf
- [43] Independent Electricity System Operator (IESO), “Yearly Hourly HOEP OR Predispatch Report,” 2018. [Online]. Available: <http://reports.ieso.ca/public/PriceHOEPPredispOR/>
- [44] Independent Electricity System Operator, “Hourly Demand Report,” 2018. [Online]. Available: <http://reports.ieso.ca/public/Demand/>
- [45] BC Hydro, “Cost calculator for energy saving,” 2019. [Online]. Available: <https://www.bchydro.com/powersmart/residential/tools-and-calculators/cost-calculator.html>
- [46] Statistics Canada, “Households and the Environment Survey 2015,” Statistics Canada, Toronto, Tech. Rep., 2016. [Online]. Available: http://sda.chass.utoronto.ca/sdaweb/dli2/hes/hes15/more_doc/HES2015_PUMF_EN_cbk.pdf
- [47] Independent Electricity System Operator, “Generator Output and Capability Report,” 2019. [Online]. Available: <http://reports.ieso.ca/public/GenOutputCapability/>
- [48] Statistics Canada, “Spending Patterns in Canada: Household equipment at the time of interview,” 2010. [Online]. Available: <https://www150.statcan.gc.ca/n1/pub/62-202-x/2008000/t011-eng.htm>